Article

TRANSPARENT PROCESS

EMBO reports

A common molecular mechanism underlies the role of Mps1 in chromosome biorientation and the spindle assembly checkpoint

Giorgia Benzi[1], Alain Camasses[2], Yoshimura Atsunori[3], Yuki Katou[3], Katsuhiko Shirahige[3] & Simonetta Piatti[1,*]

Abstract

The Mps1 kinase corrects improper kinetochore–microtubule attachments, thereby ensuring chromosome biorientation. Yet, its critical phosphorylation targets in this process remain largely elusive. Mps1 also controls the spindle assembly checkpoint (SAC), which halts chromosome segregation until biorientation is attained. Its role in SAC activation is antagonised by the PP1 phosphatase and involves phosphorylation of the kinetochore scaffold Knl1/Spc105, which in turn recruits the Bub1 kinase to promote assembly of SAC effector complexes. A crucial question is whether error correction and SAC activation are part of a single or separable pathways. Here, we isolate and characterise a new yeast mutant, *mps1-3*, that is severely defective in chromosome biorientation and SAC signalling. Through an unbiased screen for extragenic suppressors, we found that mutations lowering PP1 levels at Spc105 or forced association of Bub1 with Spc105 reinstate both chromosome biorientation and SAC signalling in *mps1-3* cells. Our data argue that a common mechanism based on Knl1/Spc105 phosphorylation is critical for Mps1 function in error correction and SAC signalling, thus supporting the idea that a single sensory apparatus simultaneously elicits both pathways.

Keywords chromosome biorientation; error correction; Mps1; Spc105; spindle assembly checkpoint

Subject Category Cell Cycle

DOI 10.15252/embr.202050257 | Received 19 February 2020 | Revised 2 March 2020 | Accepted 17 March 2020 | Published online 19 April 2020

EMBO Reports (2020) 21: e50257

Introduction

Accurate chromosome segregation is a fundamental aspect of mitosis and secures the genetic stability of a cell lineage. During the mitotic cell cycle, sister chromatids that have been generated by chromosome replication in S phase must attach through their kinetochores to microtubules emanating from opposite spindle poles in M phase. This occurs through an error correction mechanism where kinetochores dynamically attach and detach from microtubules until bipolar arrangement of sister chromatids is finalised (reviewed in ref. [1]). Bipolar attachment, also referred to as amphitelic attachment, leads to tension across kinetochores, which arises from the balance of pulling forces exerted by microtubules and counteracting forces exerted by sister chromatid cohesion (reviewed in ref. [2]). This tug of war leads also to chromosome congression to the metaphase plate.

Key to the error correction process is the evolutionary conserved CPC (chromosome passenger complex) that is composed by the Aurora B kinase and three additional centromere-targeting and activating subunits (INCENP, survivin and borealin). The CPC detects lack of kinetochore tension (e.g. in case of monotelic attachment where only one sister kinetochore is bound to microtubules or syntelic attachment where both sister kinetochores are attached to the same spindle pole) and favours amphitelic attachments by destabilising incorrect kinetochore–microtubule connections through phosphorylation of specific kinetochore substrates (reviewed in ref. [3]). The Mps1 kinase is also required for the error correction pathway in many organisms [4–8]. In human cells Mps1 acts in concert with Aurora B in this process [7,9,10]. Additionally, Mps1-specific phosphorylation targets, like the kinetochore Ska complex, have been recently involved in the error correction mechanism [11]. Importantly, in budding yeast Mps1 seems to operate independently of Aurora B in chromosome biorientation and its critical targets are unknown [6,8,12]. Although the budding yeast functional orthologue of the SKA complex, the Dam1 complex, is phosphorylated by Mps1, mutations altering these phosphorylations have no impact on chromosome segregation [12,13].

The error correction process is intimately coupled to a conserved surveillance device, the spindle assembly checkpoint or SAC, that prevents sister chromatid separation and the onset of anaphase until all chromosomes are bioriented on spindle microtubules. SAC signalling fires at unattached kinetochores, where SAC proteins are recruited, and is propagated to the whole cell for inhibition of the

1 CRBM, University of Montpellier, CNRS, Montpellier, France
2 IGMM, University of Montpellier, CNRS, Montpellier, France
3 Institute of Molecular and Cellular Biosciences, The University of Tokyo, Tokyo, Japan
*Corresponding author. Tel: +33 4343 59546; E-mail: simonetta.piatti@crbm.cnrs.fr

E3 ubiquitin ligase anaphase-promoting complex (APC) bound to its activator Cdc20. A soluble protein complex called MCC (mitotic checkpoint complex) and composed of the SAC components Bub3, BubR1, Mad2 and Cdc20 is essential for APC/Cdc20 inhibition. This, in turn, prevents degradation of APC substrates, such as securin and cyclin B, thereby halting the cell cycle before the onset of anaphase (reviewed in ref. [14]).

The Mps1 kinase acts at the apex of the SAC signalling pathway, by phosphorylating the Knl1/Spc105 kinetochore scaffold on its MELT repeats, which in turn recruit the Bub3-Bub1 SAC complex [15–18]. Subsequent binding of the SAC factor Mad1 to Bub1, together with Mps1-mediated Mad1 phosphorylation, is a prerequisite for recruitment of Mad2 to kinetochores and MCC assembly [19–23]. Consistently, phosphorylation of Knl1/Spc105 MELT repeats by Mps1 is essential for SAC signalling [15,17,18]. The Knl1/Spc105 kinetochore protein has emerged as a key factor not only as a platform for SAC signalling, but also to silence the SAC once all pairs of sister chromatids are bipolarly attached. Indeed, Knl1/Spc105 harbours at its N-terminus an "RVSF" amino acid motif that binds to PP1, which extinguishes SAC signalling at least partly by dephosphorylating Knl1/Spc105 MELT repeats [24–29]. Additionally, PP1 dephosphorylates the catalytic loop of Mps1, thus further silencing SAC [30].

Aurora B has also been implicated in SAC signalling. While an early model proposed that its role in the SAC would be indirect and linked to the generation of unattached kinetochores during the correction of tension-less kinetochore–microtubule attachments [31–34], increasing evidence supports a direct role of Aurora B in SAC activation from unattached kinetochores [9,35–39]. For instance, Aurora B promotes kinetochore recruitment of several SAC factors, including Mps1, and weakens PP1 binding to Knl1 through phosphorylation of Knl1 RVSF motif, suggesting that it acts upstream of SAC signalling [7,9,25,31,40].

The involvement of Mps1 and Aurora B in both error correction and SAC signalling raises a crucial, yet unsolved, question: are these two pathways concomitantly elicited by a common upstream sensory device or, alternatively, they respond to distinct defects (i.e. lack of kinetochore tension and lack of kinetochore attachment)? Is it possible to activate SAC without engaging the error correction machinery and vice versa? If the molecular machineries detecting these defects were separable, it should be possible to generate hypo- or hyper-morphic mutants in the two apical kinases that selectively affect either pathway without perturbing the other.

Here, we report the characterisation of a novel temperature-sensitive *mps1* mutant of budding yeast (named *mps1-3*) that is defective in chromosome biorientation and SAC signalling. An unbiased genetic screen for extragenic suppressors of the lethality of *mps1-3* cells at high temperature revealed that mutations affecting the Spc105-PP1 interface restore proper chromosome biorientation as well as a proficient SAC response. Furthermore, artificial anchoring of Bub1 near the MELT repeats of Spc105 in *mps1-3* cells results in a similar rescue. Altogether, our data indicate that Mps1 promotes both error correction and SAC signalling through a common molecular mechanism based on Spc105 phosphorylation at the MELT repeats and recruitment of the Bub1 kinase to kinetochores, thereby strengthening the idea that a single sensory apparatus engages both processes.

Results

The novel *mps1-3* mutant is defective in chromosome segregation and proficient in SPB duplication

The targets of budding yeast Mps1 in the error correction pathway are unknown so far. Dissecting the function of Mps1 in kinetochore error correction is hampered by its involvement in the duplication of spindle pole bodies (SPBs) and the assembly of a bipolar spindle [41], the first step towards chromosome biorientation.

We isolated the *mps1-3* mutant through a random mutagenesis screen for temperature-sensitive *mps1* mutants (see Materials and Methods). Haploid *mps1-3* cells grew slowly at 25–30°C and were unable to form colonies at temperatures above 32°C (Fig 1A). Sequencing of the *mps1-3* allele revealed a single mutation replacing the conserved serine 635 in the kinase domain by phenylalanine (Fig 1B). To characterise the primary defects underlying the temperature sensitivity of *mps1-3* cells, we synchronised in G1 *mps1-3* cells, together with a wild-type control and the well-characterised *mps1-1* mutant [41], and released cells at the restrictive temperature of 34°C. FACS analysis of DNA contents revealed the expected bimodal distribution of DNA contents in wild-type cells, while *mps1-3* and *mps1-1* cells showed abroad distribution of DNA contents after cytokinesis (90–105 min), indicative of massive chromosome missegregation (Fig 1C). However, while *mps1-1* cells were unable to assemble bipolar spindles due to their failure to duplicate SPBs and to activate the SAC [41], *mps1-3* cells proficiently formed bipolar spindles and elongated them during anaphase (Fig 1D and Appendix Fig S1A), suggesting that *mps1-3* might be a separation of function mutant specifically defective in chromosome biorientation but proficient at SPB duplication.

To quantify the *mps1-3* chromosome segregation defects, we used a genetic assay based on the ability of diploid cells to mate with a haploid tester strain upon events leading to loss of one of the two copies of the *MAT* locus, including loss of one entire chromosome III [42]. We used wild-type and homozygous *mps1-1/mps1-1*, *mps1-3/mps1-3* diploid cells that were grown for a defined number of generations at 25°C. Already under these permissive conditions, the appearance of mating-competent cells was 1,000- to 2,000-fold higher in the *mps1* mutants relative to the wild type (Fig 1E), suggesting pronounced chromosome III loss even in conditions that allow cell proliferation.

To follow directly chromosome biorientation in *mps1-3* haploid cells, we visualised by fluorescence microscopy the segregation of chromosome V tagged with the TetO/TetR system 1.4 kb from the centromere (*CEN5-GFP*) [43]. Cells were also expressing the SPB marker Spc97-mCherry and carried a *cdc15-2* temperature-sensitive allele to arrest cells in telophase. G1-synchronised cells were released at the restrictive temperature of 34°C, and samples were collected at 120 and 150 min from the release. As expected, near the totality of wild-type cells bioriented and properly segregated the two sister chromatids of chromosome V at opposite SPBs, while almost all *mps1-1* cells underwent *CEN5* mono-orientation on the single unduplicated SPB (Fig 1F). Strikingly, the vast majority of *mps1-3* mutant cells displayed duplicated SPBs that separated far apart, but at 120′ the two chromatids had segregated correctly to opposite spindle poles in 42% of the cells, whereas in 41% of the cells the two chromatids had remained at the same spindle pole. Only 4% of

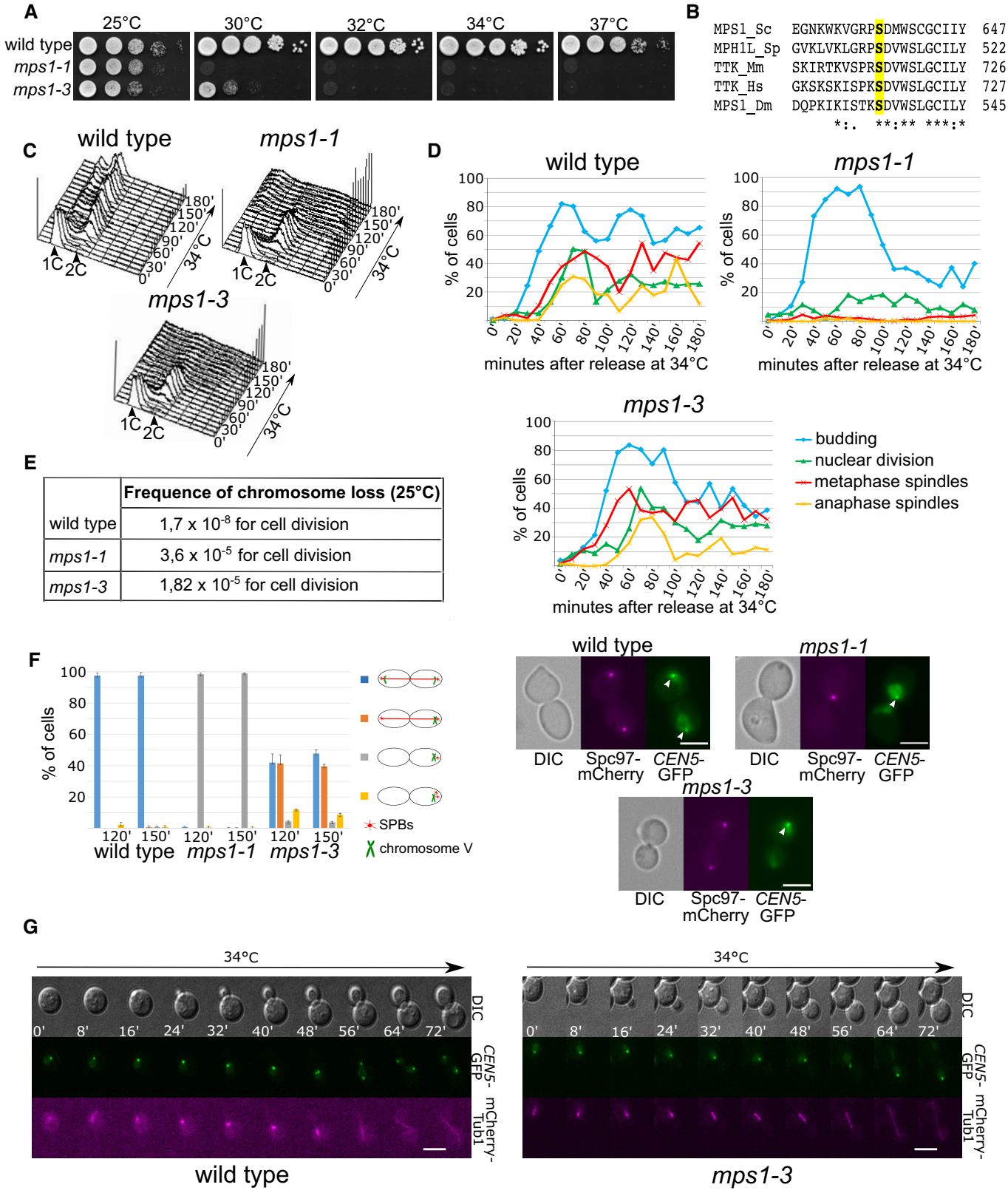
A
25°C
30°C
32°C
34°C
37°C
wild type
mps1-1
mps1-3
B
MPS1_Sc EGNKWKVGRPSDMWSCGCIIY 647
MPH1L_Sp GVKLVKLGRPSDVWSLGCILY 522
TTK_Mm SKIRTKVSPRSDVWSLGCILY 726
TTK_Hs GKSKSKISPKSDVWSLGCILY 727
MPS1_Dm DQPKIKISTKSDVWSLGCILY 545
*:. **:** ***:*
C
wild type
mps1-1
mps1-3
1C
2C
0'
30'
60'
90'
120'
150'
180'
34°C
D
wild type
mps1-1
mps1-3
% of cells
minutes after release at 34°C
budding
nuclear division
metaphase spindles
anaphase spindles
E
Frequence of chromosome loss (25°C)
wild type
1,7 x 10-8 for cell division
mps1-1
3,6 x 10-5 for cell division
mps1-3
1,82 x 10-5 for cell division
F
% of cells
120' 150' 120' 150' 120' 150'
wild type mps1-1 mps1-3
SPBs
chromosome V
wild type
mps1-1
mps1-3
DIC
Spc97-mCherry
CEN5-GFP
G
34°C
0' 8' 16' 24' 32' 40' 48' 56' 64' 72'
DIC
CEN5-GFP
mCherry-Tub1
wild type
mps1-3

Figure 1.

Figure 1. The *mps1-3* mutant is defective in chromosome biorientation.

A Serial dilutions of stationary phase cultures of the indicated strains were spotted on YEPD and incubated at the indicated temperatures.

B Mps1 sequence alignment around *Saccharomyces cerevisiae* Ser635. Sc: *Saccharomyces cerevisiae*; Sp: *Schizosaccharomyces pombe*; Mm: *Mus musculus*: Hs: *Homo sapiens*; Dm: *Drosophila melanogaster*.

C, D Wild-type, *mps1-3* and *mps1-1* mutant cells were synchronised in G1 with α-factor at permissive temperature (25°C) and then released at restrictive temperature (34°C, $t = 0$). Cells were collected at the indicated time points for FACS analysis of DNA contents (C) and for immunofluorescence using anti-tubulin antibodies in order to score metaphase and anaphase spindles (D). Budding and nuclear division were scored on the FACS samples.

E Frequencies of chromosome loss were quantified at permissive temperature (25°C).

F Wild-type and *mps1* mutant cells bearing the TetO/TetR-GFP system to mark the centromere of chromosome V [43] and expressing the SPBs marker Spc97-mCherry were synchronised as in (C, D) and arrested in anaphase through the temperature-sensitive *cdc15-2* allele. At 120 and 150 min, cells were fixed for scoring chromosome V segregation ($n \geq 172$). Arrowheads indicate the sister chromatids of chromosome V. Error bars: SD. $N = 3$. Representative images of cells for each genotype are shown on the right. Scale bar: 5 μm.

G Wild-type and *mps1-3* mutant cells carrying the TetO/TetR-GFP markers for *CEN5* labelling and expressing mCherry-Tub1 were grown at 25°C and then shifted to 34°C for 1 h before filming. Cells were filmed at 34°C every 2 min by time-lapse fluorescence microscopy. DIC: differential interference contrast. Scale bar: 5 μm.

the cells did not duplicate the SPBs, while 12% of the cells had duplicated SPBs that remained very close to each other in the mother cell, accompanied by lack of *CEN5* segregation (Fig 1F). We conclude that the *mps1-3* mutant, though capable to duplicate the SPBs and form bipolar spindles, is specifically defective in chromosome biorientation at 34°C. It is worth noting, however, that at higher temperatures (37°C) *mps1-3* cells also failed SPB duplication and bipolar spindle assembly, suggesting that *mps1-3* is a hypomorphic mutant.

Centromeric and pericentromeric cohesin is crucial for chromosome biorientation, but while centromeres transiently split in metaphase upon bipolar attachment, pericentromeric cohesion resists to pulling spindle forces [43]. We therefore asked if premature loss of pericentromeric cohesion could underlie the chromosome biorientation defect of *mps1-3* cells. To answer this question, we tagged with the TetO/TetR system the pericentromere of chromosome V (TetO array at −13 kb from the centromere ref. [43]) and analysed its behaviour in metaphase-arrested cells by fluorescence microscopy. After a pre-synchronisation in G1, cells carrying the temperature-sensitive *cdc16-1* allele (compromising APC/C activity at high temperatures and arresting cells in metaphase [44]) were released at 34°C. Under these conditions, sister pericentromeric regions of chromosome V did not disjoin in most *mps1-3* cells, similar to wild-type and *mps1-1* cells (Appendix Fig S1B). Thus, the chromosome biorientation defect of *mps1-3* cells is not explained by a premature loss of pericentric cohesion.

Biorientation defects could be due to lack of kinetochore–microtubule attachments, or to a failure in the correction of faulty kinetochore–microtubule connections that are not under tension. To discriminate between these two processes, we imaged live cells with GFP-tagged *CEN5* and expressing Tub1-mCherry to visualise microtubules. Cells were pre-incubated at 34°C for 1 h before filming at the same temperature. Under these conditions, while 100% of wild-type cells correctly bioriented the two sister *CEN5* and segregated them to opposite spindle poles ($n = 201$, Figs 1G and 3H), only 51.3% of *mps1-3* mutant cells bioriented *CEN5*, whereas 48.7% of the cells did not ($n = 179$, Figs 1G and 3H). During the whole movie, we did not detect lagging chromosomes or *CEN5* signals off the spindle in *mps1-3* cells, suggesting that kinetochore–microtubule attachment is not affected. Furthermore, in contrast to *ipl1* mutant cells that missegregate chromosomes mostly towards the old SPB [45], we found no such bias in *mps1-3* cells under the above conditions (Fig 3H). Interestingly, however, when we filmed *mps1-3* after a G1 arrest and release at 34°C (i.e. during the first cell cycle at restrictive temperature, when the pre-existing SPB is likely fully functional), we found a strong missegregation bias towards the bud (Appendix Fig S1C). This bias tends to be lost in the subsequent cell cycles (Appendix Fig S1C). From these data, we conclude that *mps1-3* cells are defective in the correction of monopolar attachments, like *ipl1* mutants and in agreement with previous conclusions [6]. Additionally, they could alter the normal pattern of SPB asymmetric inheritance (see Discussion).

The *mps1-3* mutant does not engage the spindle assembly checkpoint

To assess if *mps1-3* cells can engage the SAC, pre-synchronised G1 cells were released at 34°C in presence of the microtubule-depolymerising drug nocodazole. FACS analysis of DNA contents showed that wild-type cells arrested as expected in metaphase with 2C DNA contents, indicative of proficient SAC signalling. Contrariwise, *mps1-3* and *mps1-1* cells kept progressing through the cell cycle accumulating 4C DNA contents, indicating that they cannot engage a SAC response (Fig 2A). This was confirmed by Western blot analysis of two APC substrates, the securin Pds1 and the cyclin B Clb2, which are normally degraded in anaphase and stabilised by the SAC. As expected, both proteins remained stable in wild-type cells treated with nocodazole, while they underwent proteolysis in *mps1-1* and *mps1-3* mutants (Fig 2B). Thus, the *mps1-3* mutant is severely defective in SAC activation at high temperature.

The Mps1-3 mutant protein has enhanced kinase activity but has reduced levels at kinetochores

The catalytic activity of Mps1 is essential for both chromosome biorientation and SAC activation [5,6,8,15]. In order to understand if the defects of the *mps1-3* mutant were due to impaired Mps1 kinase activity, we performed *in vitro* kinase assays using recombinant Mps1 and Mps1-3 proteins purified from bacteria. We measured the ability of these proteins to auto-phosphorylate and to phosphorylate the N-terminal part of Spc105 (aa 1–320) at different times of incubation in the presence of $P^{33}\gamma$ATP at 34°C. Surprisingly, the Mps1-3 catalytic activity turned out to be more elevated than that of Mps1 at all time points (Fig 2C). This was confirmed by similar kinase assays in the presence of the exogenous substrate MBP and Mps1/Mps1-3 proteins affinity-purified from yeast cells using galactose-inducible glutathione *S*-transferase (GST) fusion constructs [46] (Appendix Fig S2A). Contextually, Mps1-3 protein levels in yeast

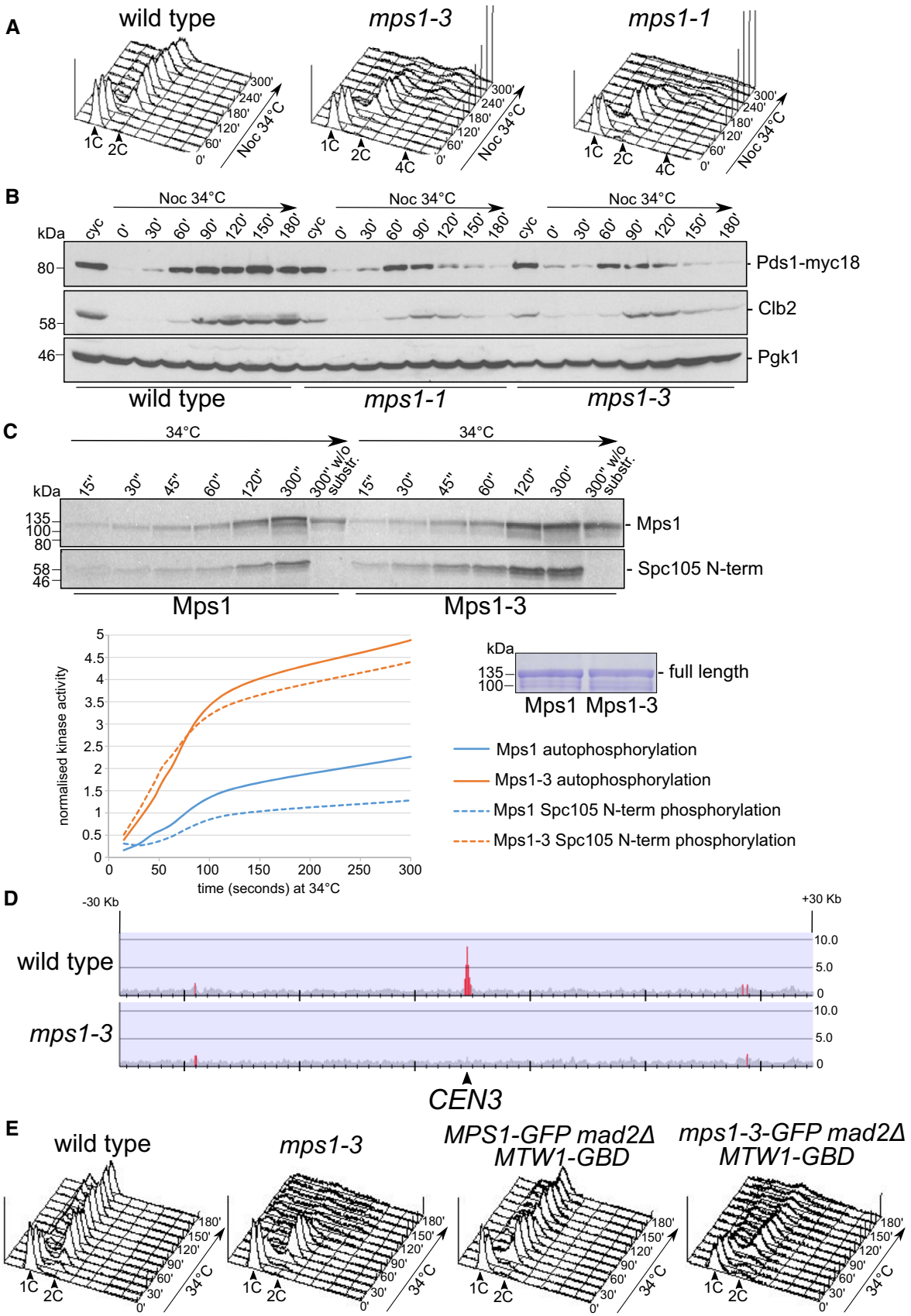
A
wild type
mps1-3
mps1-1
1C
2C
4C
0'
60'
120'
180'
240'
300'
Noc 34°C
B
Noc 34°C
kDa
cyc
0'
30'
60'
90'
120'
150'
180'
80
58
46
Pds1-myc18
Clb2
Pgk1
wild type
mps1-1
mps1-3
C
34°C
15"
30"
45"
60"
120"
300"
300" w/o substr.
135
100
80
58
46
Mps1
Spc105 N-term
Mps1
Mps1-3
normalised kinase activity
time (seconds) at 34°C
full length
Mps1 autophosphorylation
Mps1-3 autophosphorylation
Mps1 Spc105 N-term phosphorylation
Mps1-3 Spc105 N-term phosphorylation
D
-30 Kb
+30 Kb
wild type
mps1-3
10.0
5.0
0
CEN3
E
wild type
mps1-3
MPS1-GFP mad2Δ MTW1-GBD
mps1-3-GFP mad2Δ MTW1-GBD
34°C

Figure 2.

Figure 2. The *mps1-3* mutant is defective in SAC signalling and does not localise Mps1 at kinetochores.

A Wild-type and *mps1* mutant cells were synchronised in G1 with α-factor at 25°C and then released at 34°C in the presence of nocodazole (t = 0). Cells were collected at the indicated time points for FACS analysis of DNA contents.

B Cells were treated as in (A), and after 2 h from the release, α-factor was re-added to prevent cells from undergoing a second cell cycle. Cell samples were collected at the indicated time points for Western blot analysis of the indicated proteins. Pgk1 was used as loading control. Cyc: cycling cells.

C Top: *in vitro* kinase assays with recombinant Mps1 and Mps1-3 purified from *Escherichia coli* and incubated at 34°C for the indicated times in the presence of radioactive ATP and a recombinant Spc105 N-terminal fragment (aa 1–320) as substrate. Bottom left: kinase activity was quantified on the autoradiographs by ImageJ and normalised to the levels of the full-length protein on the Coomassie blue-stained gel (right). Bottom right: 1 μg of the recombinant Mps1 kinases used for kinase assays was loaded on SDS–PAGE and stained with Coomassie blue for normalisation of kinase assays.

D Wild-type and *mps1-3* cells were synchronised in G1 with α-factor at 25°C and then released at 34°C in the presence of nocodazole. Cells were collected after 90 min and fixed with formaldehyde for ChIP-seq analysis. ChIP sequence reads were normalised against sequence reads from corresponding input samples, and relative enrichment is plotted for chromosome III around the centromere (see the centromeric regions of all 16 yeast chromosomes in Appendix Fig S2). *Y*-axis shows enrichment values (linear scale, range is 0–10). Values below 1.5 are shown in grey, and values above 1.5 (i.e. sequences enriched in ChIP samples) are red coloured.

E Cells with the indicated genotypes were synchronised in G1 with α-factor at 25°C and then released in fresh medium at 34°C (t = 0). Cells were collected at the indicated time points for FACS analysis of DNA contents.

cells were also 2- to 3-fold higher than wild-type Mps1 and had aberrant electrophoretic mobility (Appendix Fig S2A). The elevated Mps1-3 levels correlated with a decreased proteolysis of the protein in mitosis (Appendix Fig S2B), consistent with the idea that Mps1 turnover inversely correlates to its kinase activity [47].

Since Mps1 levels at kinetochores increase when its kinase activity is inactivated [7,40,48–50], it is conceivable that the elevated Mps1 kinase activity in *mps1-3* cells accelerates Mps1 kinetochore turnover to a threshold that could be incompatible with SAC signalling and chromosome biorientation. To test this possibility, we tagged with three HA epitopes the *MPS1* and *mps1-3* genes at their genomic locus and checked the distribution of the corresponding proteins on chromosomes by ChIP-seq using cells pre-synchronised in G1 and released in nocodazole for 90 min at 34°C, time at which both *MPS1* and *mps1-3* cells were still in mitosis. Strikingly, while wild-type Mps1 clearly accumulated at the centromeric region of all 16 yeast chromosomes, Mps1-3 did not (Fig 2D and Appendix Fig S3), suggesting that its residence at kinetochores is severely impaired.

To definitely ascertain if reduced kinetochore levels are the main reason for the Mps1-3 loss of function, we artificially recruited to kinetochores GFP-tagged Mps1 and Mps1-3 in cells that co-expressed the kinetochore protein Mtw1 tagged with the high affinity GFP-nanotrap (GFP-binding domain or GBD) [51]. This strategy led to constitutive association of Mps1 to the kinetochore in 91.3% of the cells and of Mps1-3 in 88.5% of the cells (n = 196 and n = 209, respectively). Cells also carried the deletion of *MAD2* to obliterate SAC, which would be otherwise constitutively active following Mps1 tethering to kinetochores [49,52]. Notably, anchoring Mps1-3 to Mtw1 could partially restore proper chromosome segregation at 34°C, as shown by the bimodal distribution of DNA contents by FACS analysis (Fig 2E), suggesting that the chromosome biorientation defects of *mps1-3* cells are largely accounted for by decreased Mps1 kinetochore levels.

A genetic screen for spontaneous suppressors of the *mps1-3* mutation

Since SAC is not essential in budding yeast [53,54], we reasoned that chromosome missegregation could be the main cause of the lethality of *mps1-3* cells at high temperatures, which makes this mutant a unique genetic tool to study the role of Mps1 in chromosome biorientation. To gain insights into this process, we performed an unbiased genetic screen for spontaneous mutations suppressing the temperature sensitivity of *mps1-3* cells at 34°C. Classical genetic analyses allowed us to establish if the suppressing mutations were recessive or dominant, distinguish the intragenic from the extragenic suppressors (i.e. suppressing mutation inside or outside the *mps1-3* gene, respectively) and assess if the extragenic suppressors were allelic to one another. Through this screen, we could isolate 27 suppressors. Out of these, 17 turned out to be intragenic while 10 were extragenic suppressors. We focused on the extragenic suppressors, which could provide valuable insights into the molecular mechanism underlying the role of Mps1 in chromosome biorientation. Through genetic analyses and whole genome sequencing, we could establish that the suppressing mutations hit three different genes (Fig 3A and B): *SPC105*, encoding for the kinetochore protein Spc105/Knl1; *GLC7*, encoding for the catalytic subunit of the phosphatase PP1; and *GRR1*, encoding for an F-box protein of the E3 ubiquitin ligase complex SCF. Three *GRR1* suppressors out of four carried also a mutation in *RSC30*, encoding for a subunit of the RSC chromatin-remodelling complex [55]. The basis for the suppression by the *GRR1* mutations, alone or in combination with the mutation in *RSC30*, was not immediately clear and will be investigated in the future.

Spc105 (Knl1 in metazoans) is a known target of Mps1 in the SAC [15]. Mps1-dependent phosphorylation of its MELT repeats is crucial for SAC signalling by recruiting Bub1 and Bub3 [15–18]. The PP1 Glc7 in turn dephosphorylates Spc105 MELT repeats by binding directly the consensus RV/IXF motif at the N-terminus of Spc105 (RVSF, aa 75–78) to release Bub1 and silence the checkpoint [15,28]. Strikingly, all our suppressing mutations in *SPC105* encompassed or were close to the PP1-binding motif, while both *GLC7* suppressors carried a missense mutation of Phe256 (to Ile or Val), which resides in the hydrophobic groove involved in PP1 interaction with partners carrying the RV/IXF consensus motif [56] (Fig 3B). Collectively, these observations suggest that reduced PP1 interaction with Spc105 likely accounts for the rescue of the temperature sensitivity of *mps1-3* cells. Interestingly, the *spc105-V76G* mutation was recessive and lethal in otherwise wild-type cells, consistent with the notion that mutations in the PP1-binding site of Spc105 are inviable due to constitutive SAC activation [28], while *spc105-A79T* and *spc105-V82D* were viable, suggesting that they might interfere with PP1 recruitment to kinetochores less severely than *spc105-V76G*. It is also worth noting that *spc105-V76G* suppressed more robustly than *spc105-A79T* and *spc105-V82D* the lethality of *mps1-3* cells at high temperatures (Fig 3A).

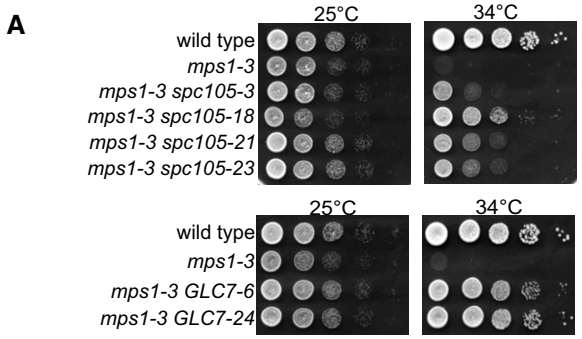

B

Suppressor	Gene	Aminoacid substitution
3	*SPC105*	Ala79Thr
18	*SPC105*	Val76Gly
21,23	*SPC105*	Val82Asp
6	*GLC7*	Phe256Ile
24	*GLC7*	Phe256Val
17	*GRR1* *RSC30*	Ser772Pro Gly571Asp
19	*GRR1* *RSC30*	Asn1069Lys Gly571Asp
20	*GRR1*	Ser772Pro
26	*GRR1* *RSC30*	Cys730Trp Gly571Asp

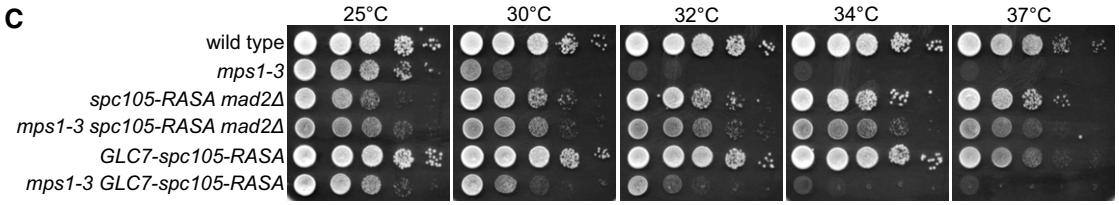

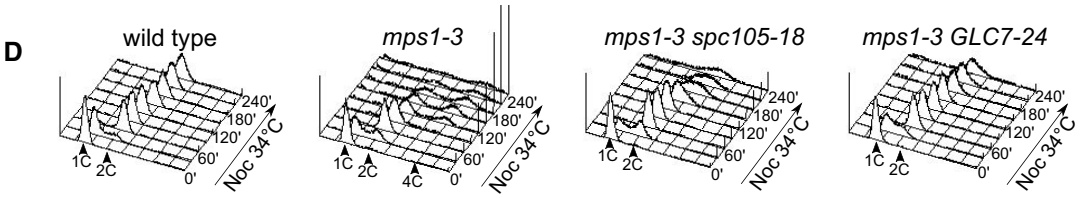

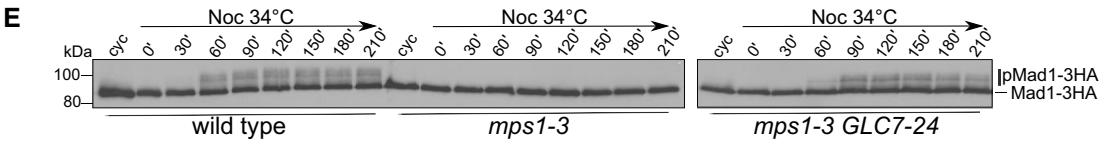

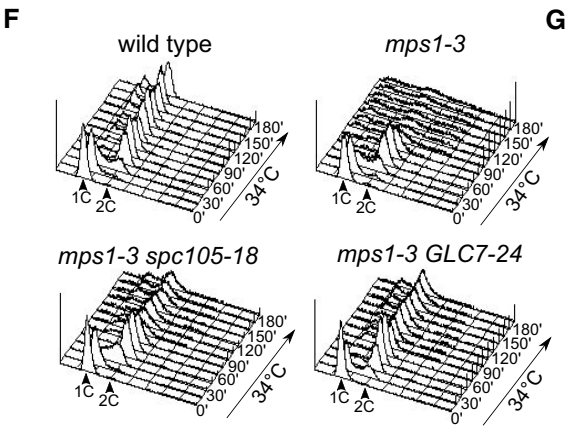

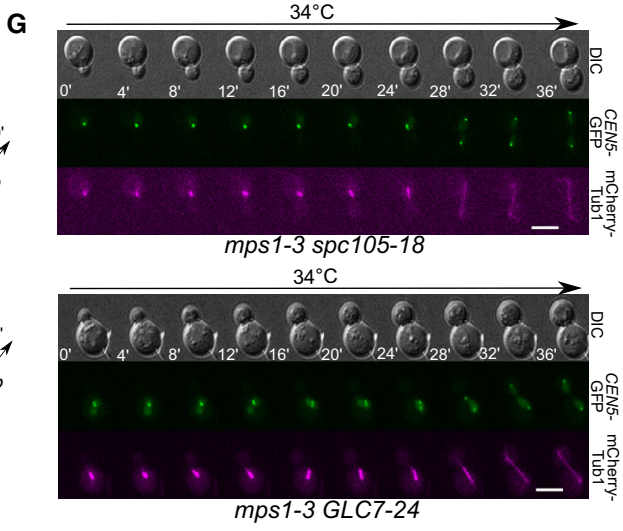

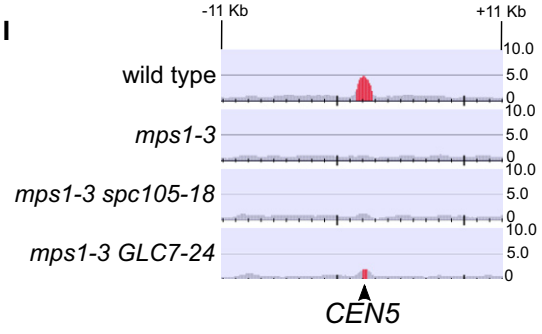

H

T= 34°C	normal segregation	missegregation		n
		mother	bud	
wild type	100%	/	/	201
mps1-3	51.3%	26.3%	22.4%	179
mps1-3 spc105-18	96.2%	0.3%	3.5%	341
mps1-3 GLC7-24	98.5%	0.4%	1.1%	272
mps1-3 spc105-18 mad2Δ	93.4%	3.5%	3.1%	198
mps1-3 GLC7-24 mad2Δ	92.7%	3.9%	3.5%	281

Figure 3.

Figure 3. Characterisation of the extragenic suppressors of *mps1-3* mutant cells.

A Serial dilutions of stationary phase cultures of the indicated strains were spotted on YEPD and incubated at 25°C and 34°C.

B List of extragenic suppressors found in the unbiased genetic screen.

C Serial dilutions of stationary phase cultures of the indicated strains were spotted on YEPD and incubated at the indicated temperatures.

D Cells with the indicated genotypes were synchronised in G1 with α-factor at 25°C and then released in fresh medium at 34°C in presence of nocodazole (t = 0). Cells were collected at the indicated time points for FACS analysis of DNA contents.

E Cells were treated as in (D) and collected at the indicated time points for Western blot analysis of Mad1-3HA. Cyc: cycling cells.

F Cells with the indicated genotypes were synchronised at 25°C and then released in fresh medium at 34°C (t = 0). Cells were collected at the indicated time points for FACS analysis of DNA contents.

G, H Cells with the indicated genotypes carrying the TetO/TetR-GFP markers for *CEN5* labelling and expressing mCherry-Tub1 were grown at 25°C and then shifted to 34°C for 1 h before filming. Cells were filmed at 34°C every 2 or 4 min by time-lapse fluorescence microscopy. Chromosome V segregation errors are reported in the table (H). Representative cells are shown as examples in the montages (G). Representative montages for wild-type and *mps1-3* cells are shown in Fig 1F. DIC: differential interference contrast. Scale bar: 5 μm.

I Wild-type, *mps1-3*, *mps1-3 spc105-18* and *mps1-3 GLC7-24* cells were synchronised in G1 with α-factor at 25°C and then released at 32°C in the presence of nocodazole (note that the presence of 3HA tags at the C-terminus of Mps1-3 slightly decreases the maximal temperature of suppression). Cells were collected after 90 min and fixed with formaldehyde for ChIP-seq analysis. ChIP sequence reads were normalised against sequence reads from corresponding input samples, and relative enrichment is plotted for chromosome III around the centromere (see the centromeric regions of all 16 yeast chromosomes in Appendix Fig S5). Y-axis shows enrichment values (linear scale, range is 0–10). Values below 1.5 are shown in grey, and values above 1.5 (i.e. sequences enriched in ChIP samples) are red coloured.

Consistent with the idea that lack of PP1 recruitment to Spc105 rescues the lethality of *mps1-3* cells, the well-characterised *RASA* mutation in the PP1 binding motif of Spc105 [28] also suppressed the temperature sensitivity of *mps1-3* cells (Fig 3C; note that the *spc105-RASA* mutation is lethal unless SAC activity is abolished, e.g. by *MAD2* deletion [28]). Additionally, fusing the PP1 catalytic subunit Glc7 to the N-terminus of the Spc105-RASA mutant protein [28] almost completely abolished its suppressing properties (Fig 3C), indicating that suppression stems only from loss of PP1 binding to Spc105.

The *GLC7* mutations isolated in our screen were dominant and viable in otherwise wild-type cells. Since dominant mutations are often associated with gain of function, this observation was quite puzzling and prompted us to characterise PP1 activity in *GLC7-24* cells. As a readout, we analysed the phosphorylation status of the well-characterised PP1 cytoplasmic substrate Snf1, which is hyperphosphorylated on T210 under low glucose conditions (1%) and gets dephosphorylated by Glc7 in high glucose (4%) [57]. No significant differences in the phosphorylation of Snf1 T210 were apparent in *mps1-3 GLC7-24* and *GLC7-24* cells relative to the wild type (Appendix Fig S4A), suggesting that the cytoplasmic activity of PP1 is not affected. To assess PP1 phosphatase activity at kinetochores in *GLC7-24* cells, we monitored phosphorylation of Sli15, a subunit of the Aurora B complex that resides at kinetochores and on spindle microtubules and is involved in chromosome biorientation [45,58]. Sli15 is phosphorylated by Ipl1/Aurora B [59], whose activity is often reversed by PP1 [60,61]. Interestingly, Sli15 phosphorylation was more pronounced in cycling cells and slightly advanced during the cell cycle in the *GLC7-24* mutant relative to the wild type (Appendix Fig S4B). Thus, Glc7 phosphatase activity is not globally elevated in *GLC7-24* cells; rather, it might impair dephosphorylation of specific kinetochore substrates.

Suppressing mutations in *SPC105* and *GLC7* restore SAC activation and normal chromosome segregation in *mps1-3* cells

To investigate further the phenotypes of the suppressors, we analysed their ability to engage the SAC and undergo normal chromosome segregation. Pre-synchronised G1 cells were released at 34°C in the presence and absence of nocodazole and subjected to FACS analysis of DNA contents at different time points. Importantly, the *spc105-18* and *GLC7-24* mutations restored proficient SAC activation in *mps1-3* cells (Fig 3D). In *mps1-3 GLC7-24* cells, this was accompanied by Mad1 hyperphosphorylation, which requires Mps1 activity [62,63] and was abolished in *mps1-3* cells (Fig 3E; note that we could not study Mad1 phosphorylation pattern in *mps1-3 spc105-18* cells due to their synthetic lethality with HA-tagged Mad1). Since Mad1 is recruited to unattached kinetochores and is not part of soluble MCC [64,65], these data further strengthen the idea that in *GLC7-24* cells PP1 has impaired ability to dephosphorylate kinetochore substrates. Additionally, they raise the possibility that PP1 could dephosphorylate Mad1 directly.

Remarkably, the *spc105-18* and *GLC7-24* suppressors also rescued the chromosome segregation defects of *mps1-3*, as shown by the bimodal distribution of DNA contents after one complete cell cycle at 34°C (Fig 3F). Moreover, live cell imaging of *mps1-3 spc105-18* and *mps1-3 GLC7-24* cells with GFP-tagged *CEN5* and expressing Tub1-mCherry showed nearly complete suppression of chromosome missegregation (Fig 3G and H). Importantly, the *spc105-18* and *GLC7-24* alleles did not restore normal levels of Mps1-3 at centromeres, as shown by ChIP-seq (Fig 3I and Appendix Fig S5). Furthermore, suppression of chromosome missegregation was not a consequence of restored SAC activity, which might impose sufficient time for error correction, because it remained unchanged upon *MAD2* deletion (Fig 3H).

Thus, these data strongly argue that a common mechanism involving Mps1 and antagonised by PP1 simultaneously promotes error correction of faulty kinetochore attachments and SAC signalling.

The *spc105-18* and *GLC7-24* suppressors restore Spc105 phosphorylation in *mps1-3* cells

To further explore the possibility that Mps1 could promote SAC signalling and chromosome biorientation through the same molecular mechanism, we analysed the phosphorylation status of Spc105 in wild-type and *mps1-3* cells at 34°C in presence or absence of nocodazole. As expected, Spc105 tagged with 3HA (Spc105-3HA) was promptly phosphorylated in wild-type cells treated with nocodazole, as indicated by its mobility shift in SDS–PAGE (times

60–150 min after release from G1, Fig 4A). Phosphorylation was impaired in *mps1-3* cells under the same conditions, in agreement with the notion that Spc105 is a critical Mps1 substrate during SAC activation [15]. Importantly, Spc105 phosphorylation was efficiently restored, if not accentuated, in the *mps1-3 spc105-18* and *mps1-3 GLC7-24* mutants (Fig 4A), consistent with defective PP1 activity at kinetochores that counteracts Mps1-dependent phosphorylation of Spc105 during SAC signalling. Interestingly, we could detect a slight electrophoretic mobility shift of Spc105 also in wild-type cells undergoing a normal cell cycle in the absence of nocodazole (Fig 4B, times 30′–40′ after release from G1, which corresponds to cells in S phase), suggesting that Mps1 might phosphorylate a low number of MELT repeats in unperturbed conditions. Consistent with this hypothesis, an unphosphorylatable MELT mutant (*spc105-6A*) is unable to recruit Bub1 to kinetochores also during unperturbed conditions and displays chromosome segregation defects [15]. Spc105 phosphorylation was not apparent in *mps1-3* cells at 34°C and was restored in *mps1-3 spc105-18* cells (Fig 4B). It is worth noting that the mobility shift of Spc105 was even more conspicuous and present for a larger cell cycle window in *mps1-3 spc105-18* cells

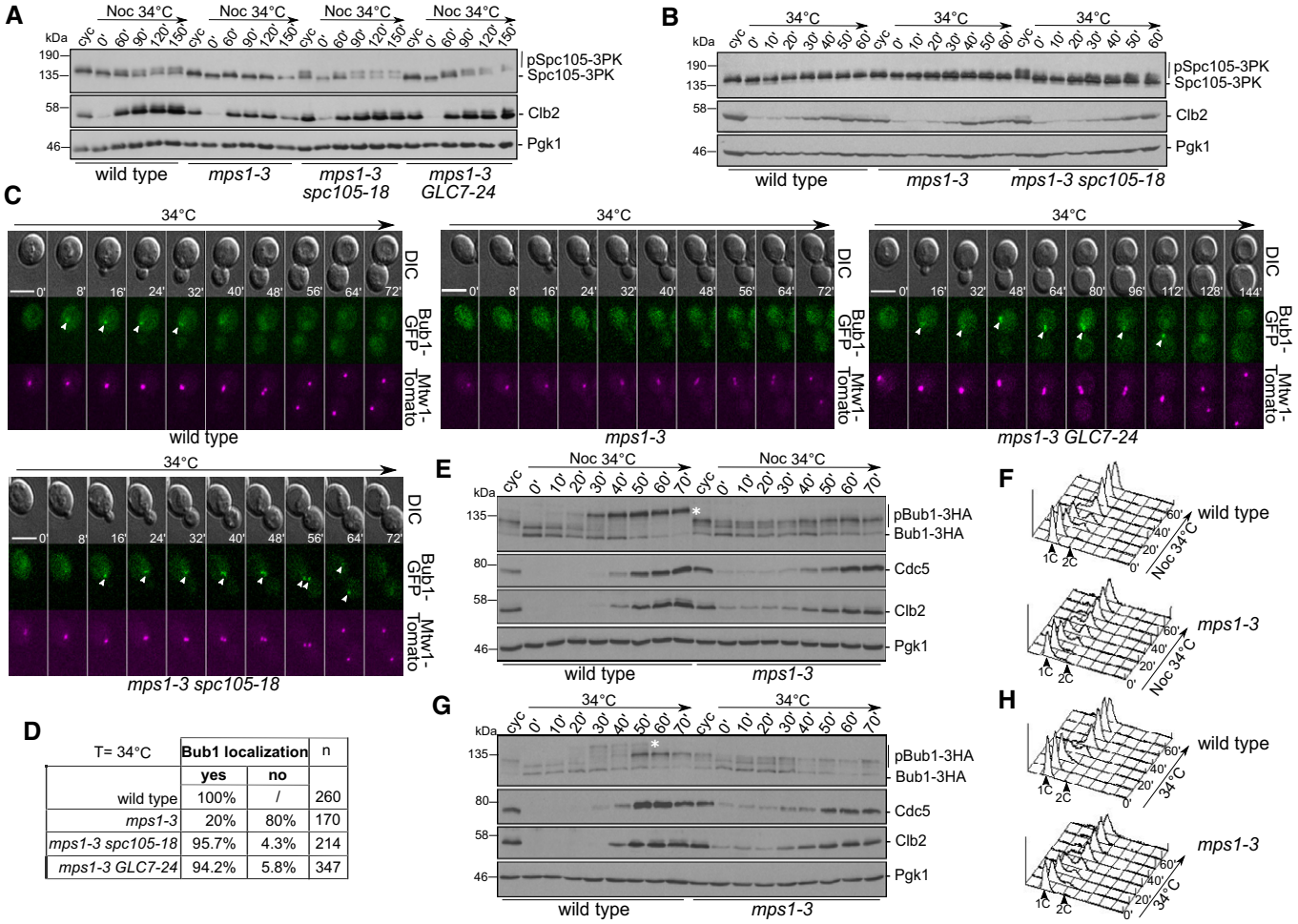

T= 34°C	Bub1 localization		n
	yes	no	
wild type	100%	/	260
mps1-3	20%	80%	170
mps1-3 spc105-18	95.7%	4.3%	214
mps1-3 GLC7-24	94.2%	5.8%	347

Figure 4. Spc105 phosphorylation and Bub1 kinetochore recruitment are impaired in *mps1-3* cells.

A, B Wild-type and *mps1-3* cells were synchronised in G1 with α-factor at 25°C and then released at 34°C in the presence (A) or absence (B) of nocodazole (t = 0). Cells were collected at the indicated time points for Western blot analysis of the indicated proteins. Equal amounts of protein extracts were loaded on two different gels, for Western blot of Spc105-3PK and Clb2/Pgk1, respectively. Clb2 was used as mitotic marker and Pgk1 as loading control. Cyc: cycling cells.

C, D Cells with the indicated genotypes expressing Bub1-GFP and the kinetochore marker Mtw1-Tomato were grown in SD glu 2% and then shifted to 34°C for 1 h before filming; they were then filmed every 4 min by time-lapse fluorescence microscopy at 34°C. Note that *BUB1-GFP* is synthetic lethal with *mps1-3*. Thus, we used *mps1-3 GALs-MPS1 BUB1-GFP* cells that were grown in -His RG medium at 30°C; glucose was added to the culture for 30 min to shut off *GALs-MPS1*, followed by shifting cells to SD medium at 34°C for 1 h before imaging in the same medium. Montages show representative cells (C). Arrowheads indicate Bub1-GFP signals at kinetochores. DIC: differential interference contrast. Scale bar: 5 μm. GFP signals (Bub1) co-localising with Tomato signals (kinetochores) were scored on the movies (D).

E–H Wild-type and *mps1-3* cells were synchronised in G1 with α-factor at 25°C and then released at 34°C in the presence (E, F) or absence (G, H) of nocodazole (t = 0). Cells were collected at the indicated time points for Western blot analysis of the indicated proteins (E, G) and for FACS analysis of DNA contents (F, H). Equal amounts of protein extracts were loaded on two different gels, for Western blot of Bub1-3HA/Cdc5 and Clb2/Pgk1, respectively. A white asterisk indicates a hyperphosphorylated isoform of Bub1 that in wild-type cells correlates with lack of chromosome biorientation. Cdc5 and Clb2 were used as mitotic markers and Pgk1 as loading control. Cyc: cycling cells.

than in the wild type (Fig 4B), in line with the impaired PP1 activity at Spc105 in this mutant. Moreover, it was prominent in *mps1-3 spc105-18* cells at 25°C, but less so at 34°C (Appendix Fig S6A), confirming that it depends on Mps1 activity at kinetochores.

Bub1 recruitment to kinetochores is impaired in *mps1-3* cells but is restored by the *spc105-18* and *GLC7-24* suppressing mutations

As mentioned above, Spc105/Knl1 phosphorylation primes Bub1 recruitment to kinetochores for SAC signalling [15–18]. Since Bub1 transiently associates with kinetochores also under unperturbed conditions [65], we visualised by time-lapse video microscopy Bub1-GFP along with the kinetochore marker Mtw1-Tomato in wild-type and *mps1-3* cells at 34°C. Under these conditions, Bub1 was transiently recruited to kinetochores in wild-type cells with a small and medium bud, i.e. during S phase and early mitosis, in 100% of the cells (n = 260, Fig 4C and D). In *mps1-3* cells, we detected low levels of Bub1 at kinetochores only in 20% of the cells at 34°C (n = 170, Fig 4C and D), while the protein co-localised normally with Mtw1 in small- and medium-budded cells at 25°C (Appendix Fig S6B). Therefore, lack of Spc105 phosphorylation in *mps1-3* cells under unperturbed conditions correlates with loss of Bub1 at kinetochores. Remarkably, Bub1 kinetochore localisation was restored to nearly wild-type levels in *mps1-3 spc105-18* and *mps1-3 GLC7-24* cells (Fig 4C and D), further strengthening the correlation between Spc105 phosphorylation and Bub1 residence at kinetochores. It is worth noting that while in wild-type cells Bub1 dissociated from the kinetochores at the time of chromosome biorientation, it persisted at kinetochores up to anaphase in the majority of *mps1-3 spc105-18*, in good agreement with Spc105 hyperphosphorylation in these cells.

In order to be fully functional for SAC activation, Bub1 also needs to be directly phosphorylated by Mps1, which in turn allows its binding to Mad1 [19–21]. Thus, we checked if Bub1 phosphorylation was also impaired in *mps1-3* cells. Pre-synchronised G1 cells were released at 34°C in the presence or the absence of nocodazole. Although several forms of Bub1 with different electrophoretic mobility were present throughout the cell cycle, one particular isoform with slowest mobility appeared in the wild type at 20′ after G1 release, i.e. when cells entered S phase, thus correlating with the timing of Bub1 kinetochore localisation (Fig 4E–H). While this hyperphosphorylation was transient in the absence of nocodazole, disappearing by 60′ (Fig 4G), it accumulated upon microtubule depolymerisation in wild-type cells (Fig 4E). Under both conditions, this isoform was not apparent in *mps1-3* cells, suggesting that it is phosphorylated by kinetochore-bound Mps1 (Fig 4E and G). Furthermore, Bub1 hyperphosphorylation was not restored in the *mps1-3 spc105-18* and *mps1-3 GLC7-24* suppressors undergoing cell cycle progression in the absence (Appendix Fig S6C) or in the presence of nocodazole (Appendix Fig S6D), although a modest Bub1 hyperphosphorylation could be observed in the *mps1-3 GLC7-24* suppressor treated with nocodazole at late time points (Appendix Fig S6D). Thus, the mechanism underlying the suppression of *mps1-3* mutant cells might be independent of the phosphorylation status of Bub1.

Since Bub1 has been involved in kinetochore biorientation in budding yeast [8,66], we conclude that lack of Bub1 recruitment to kinetochores is likely the main reason underlying the chromosome segregation defects of *mps1-3* cells. Lowering PP1 levels at Spc105 in the suppressors favours phosphorylation of the MELT repeats of Spc105, thereby restoring Bub1 recruitment at kinetochores and chromosome biorientation.

Artificial targeting of Bub1 to Spc105 restores proper chromosome segregation and SAC response in *mps1-3* cells

If our above conclusions are correct, artificial tethering of Bub1 to kinetochores could rescue the chromosome segregation defects of *mps1-3* cells at high temperatures. To test this hypothesis, we generated yeast strains expressing as sole source of Spc105 an Spc105 variant where we had inserted the GFP-binding domain upstream of the MELT repeats of Spc105 (Spc105-GBD). In the same strains, we co-expressed Bub1-GFP or Bub3-GFP (note that although Bub3 enhances Bub1 binding to Spc105 by directly reading its phosphorylated MELT repeats, it has no additional role in Bub1 activation [16,67]). This strategy led to constitutive recruitment of Bub1 to kinetochores throughout the cell cycle (Fig 5A and Movie EV1), with no obvious impact on the proliferation rate of otherwise wild-type cells (Fig 5B), indicating that prolonged Bub1 residence at kinetochores is insufficient to constitutively activate the SAC. Artificial recruitment of Bub1 to Spc105 only modestly, if at all, rescued the lethality of *mps1-3* cells at high temperatures (Fig 5B). However, it did prolong the viability of *mps1-3* cells after transient incubation at restrictive temperature (Fig 5C), suggesting that proper chromosome segregation might be partially restored. In agreement with this hypothesis, FACS analysis of DNA contents in synchronised *mps1-3* cells, either lacking or carrying the *SPC105-GBD* and *BUB1-GFP* or *BUB3-GFP* constructs, showed that the massive chromosome missegregation of *mps1-3* cells at 34°C was partially (*BUB3-GFP*) or largely (*BUB1-GFP*) rescued, as indicated by the bimodal distribution of DNA contents (Appendix Fig S7A and Fig 5D). Interestingly, artificial anchoring of Bub1 to Spc105 also partially suppressed the SAC defects of *mps1-3* cells (Appendix Fig S7B). Nevertheless, the rescue of chromosome missegregation was independent of restored SAC signalling, as it remained unaffected by *MAD2* deletion (Fig 5C and D). Thus, the main reason underlying the chromosome biorientation, and possibly SAC defects, of *mps1-3* cells is the lack of Bub1 at kinetochores.

The function of Mps1 and Bub1 in chromosome biorientation has been previously linked to pericentromeric localisation of Shugoshin, which in yeast requires Mps1 and Bub1 kinase activity [10,66,68,69]. Shugoshin senses the lack of kinetochore tension and engages the error correction machinery through kinetochore recruitment of the CPC complex (chromosome passenger complex) [68–74]. Although the role of budding yeast Mps1 in chromosome biorientation seems independent of the CPC and Aurora B activity [6,8], we decided to investigate if the chromosome segregation defects of *mps1-3* cells could be ascribed to poor Shugoshin activity at pericentromeres. Although co-localisation of Sgo1 (the only budding Shugoshin) with kinetochore clusters was partially compromised in *mps1-3* cells at 34°C (Appendix Fig S8A), in agreement with previous observations [8] and with the loss of Bub1 at kinetochores, *mps1-3* cells turned out to be synthetically lethal with *SGO1* deletion even at 25°C (Appendix Fig S8B), strongly arguing against a linear pathway where Mps1 acts upstream of Sgo1.

The role of budding yeast Aurora B (Ipl1) in chromosome biorientation relies on its alternative targeting to centromeres or the

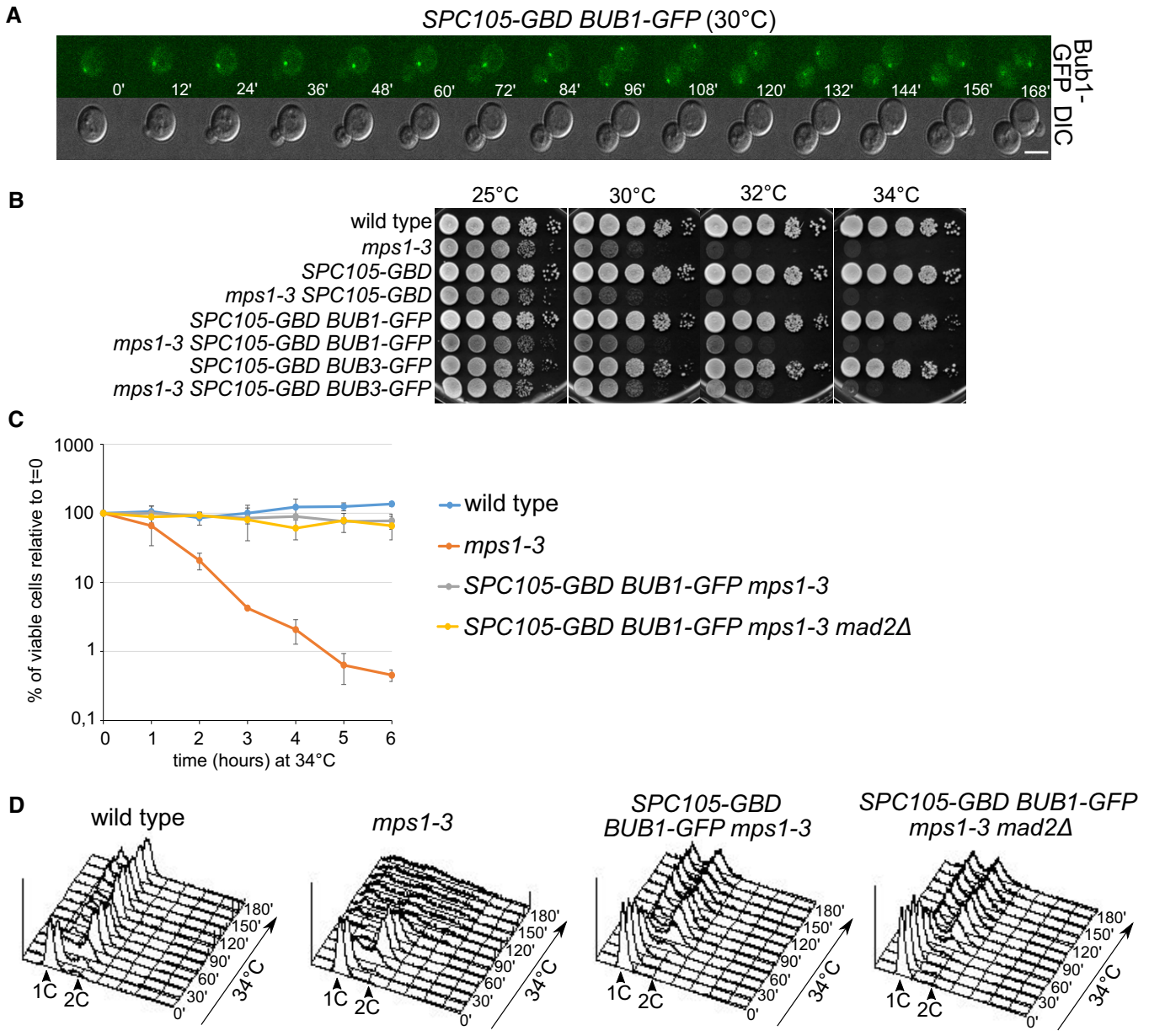

Figure 5. Artificial recruitment of Bub1 to Spc105 is sufficient to suppress the chromosome biorientation defects of *mps1-3* cells.

A *SPC105-GBD* cells expressing Bub1-GFP were grown at 30°C and filmed every 4 min at 30°C by time-lapse fluorescence microscopy. DIC: differential interference contrast. Scale bar: 5 μm.

B Serial dilutions of stationary phase cultures of the indicated strains were spotted on YEPD and incubated at the indicated temperatures.

C Cells with the indicated genotypes were grown at 25°C and then shifted at 34°C (t = 0). Every hour after the temperature shift, the same number of cells was plated on YEPD for each strain and incubated at 25°C to determine the number of colony-forming units. Percentages of viable cells have been calculated for each strain relative to t = 0. Error bars: SD. N = 3.

D Cells with the indicated genotypes were synchronised in G1 with α-factor at 25°C and then released in fresh medium at 34°C. Cells were collected at the indicated time points for FACS analysis of DNA contents.

inner kinetochore [75–77]. While centromeric localisation depends on histone H2A phosphorylation by Bub1 and subsequent recruitment of Shugoshin and the Bir1 subunit of CPC (survivin in metazoans) [71,77,78], kinetochore localisation requires binding of Aurora B and the Sli15 subunit of CPC (INCENP in metazoans) to the COMA complex [75,77]. A truncated Sli15 lacking its N-terminal region (Sli15-ΔNterm) or alanine mutations in its CDK-dependent phosphorylation sites (Sli15-6A) might favour Ipl1 binding to the COMA complex and/or microtubules [75,77,79] and, concomitantly, rescue the lethality/growth defects of *bir1Δ*, *bub1Δ* and *sgo1Δ* cells [80]. If the chromosome segregation defects of *mps1-3* cells arose exclusively from poor activity of centromeric Sgo1/CPC, then they

should be similarly suppressed by the Sli15-ΔNterm and Sli15-6A variants. This was definitely not the case, as shown by proliferation assays (Appendix Fig S8C) and FACS analysis of DNA contents on synchronised cells (Appendix Fig S8D).

Finally, since Dam1 is a critical phosphorylation target of Ipl1 in the error correction process [12,81], we monitored its phosphorylation state in wild-type, *mps1-3* and *ipl1-321* cells during a synchronous release from G1 at 34°C. While the electrophoretic mobility of Dam1-3PK was dramatically altered by the *ipl1-321* mutation, it was mainly unaffected in *mps1-3* cells (Appendix Fig S8E), consistent with the notion that phosphorylation of Dam1 by Mps1 is dispensable for chromosome biorientation [12,13] and suggesting that Ipl1 kinase activity is largely proficient in *mps1-3* cells.

We therefore conclude that lack of Bub1 at kinetochores is mainly responsible for the chromosome biorientation flaws of *mps1-3* mutant cells, at least partly independently of the role of Bub1 in Sgo1 kinetochore recruitment and CPC activation.

Discussion

The *mps1-3* mutant as a novel genetic tool to study the role of Mps1 in chromosome segregation

The precise function of budding yeast Mps1 in chromosome biorientation has been elusive so far. We have shed light on this process through the characterisation of the conditional *mps1-3* mutant that at 34°C is defective in this process but proficient at SPB duplication and bipolar spindle assembly. Our analysis of the segregation pattern of chromosome V in *mps1-3* cells suggests that each pair of sister chromatids has equal chance to segregate in a bipolar or monopolar fashion. This random segregation applied to the 16 yeast chromosomes makes the likelihood for each single *mps1-3* cell to segregate correctly all chromosomes extremely low (1.5×10^{-5}), which is in agreement with the massive chromosome missegregation we observe by FACS analysis. Being *mps1-3* cells also SAC-deficient makes monopolar attachments undetected by the checkpoint, thus generating highly aneuploid cells.

We could establish through live cell imaging that *mps1-3* cells are not defective in kinetochore–microtubule attachment, but rather in the error correction mechanism that converts monotelic or syntelic linkages into amphitelic attachments, in agreement with previous conclusions [6,8]. This function has been classically attributed to Aurora B and the CPC (reviewed in ref. [82]), but in more recent years Mps1 has also been implicated in this process. Mps1 was shown to impact on Aurora B activity through phosphorylation of the CPC subunit borealin [4], as well as to act downstream of Aurora B [7], suggesting a complex interplay between the two kinases. In contrast, in budding yeast Mps1 and Aurora B (Ipl1) were proposed to operate independently [6,8].

While *ipl1* mutants missegregate chromosomes preferentially towards the old SPB, presumably because the new SPB must undergo a maturation time before becoming fully able to nucleate microtubules [45], we find different results in *mps1-3* cells depending on the experimental conditions. In particular, during the first cell cycle at restrictive temperature *mps1-3* cells missegregate chromosomes preferentially towards the bud (i.e. towards the old SPB) similar to *ipl1* mutant cells. In contrast, during the following cell cycles this bias seems to be progressively lost. These results can be rationalised by surmising that Mps1 and Ipl1 are both involved in error correction of kinetochore attachments, but Mps1 could be additionally required for SPB maturation. In other words, when Mps1 activity is disabled, young SPBs fail to age properly and SPB asymmetry is obliterated, thus explaining the loss of missegregation bias after the second cell cycle at restrictive temperature. It is worth noting that apparently contradictory data exist in the literature as to whether in *mps1* mutants chromosomes missegregate preferentially towards the bud [5,6,83]. The above hypothesis offers a plausible explanation to reconcile these data.

Although the *mps1-3* Ser635Phe mutation lies in the kinase domain, the *in vitro* kinase activity of the corresponding protein is surprisingly enhanced, rather than impaired, at high temperature. The crystal structure of the Mps1 kinase domain has been solved [84] and reveals that Ser635 is semi-buried, thus precluding any straightforward prediction of the possible outcome of its mutation on Mps1 folding or activity. Importantly, the Mps1-3 protein does not accumulate at kinetochores, suggesting that lack of phosphorylation of specific kinetochore substrates underlies the chromosome biorientation and SAC defects of *mps1-3* cells. For what concerns SAC signalling, although *MPS1* overexpression is able to hyperactivate SAC in the absence of functional kinetochores [85], our data imply that endogenous levels of Mps1 must accumulate at kinetochores for a productive SAC response, in agreement with previous reports [9,86–88]. Mps1 kinetochore recruitment depends on its N-terminus that interacts with the kinetochore protein Ndc80/Hec1 [86,87]. Additionally, Mps1 kinase activity promotes its own turnover at kinetochores [7,40,49,50]. It is therefore tempting to speculate that the enhanced kinase activity of Mps1-3 might accelerate its own turnover and account for its low levels at kinetochores. The characterisation of the intragenic suppressors identified in our genetic screen might help shedding light on this hypothesis.

Mps1 promotes SAC signalling and chromosome biorientation through a common molecular mechanism

Our unbiased screen for extragenic suppressors of *mps1-3* has been particularly revealing and points at the antagonism between Mps1 and PP1 at kinetochores as critical for the correction of faulty kinetochore–microtubule attachments and correct chromosome segregation. Our data strongly argue that the same mechanism implicated in SAC signalling, i.e. Spc105 phosphorylation and subsequent Bub1 recruitment, is a crucial function of Mps1 also in chromosome biorientation and independently of SAC activation. Several lines of evidence are consistent with this conclusion. First, the *spc105* and *GLC7* suppressors that we have identified can re-establish both proper chromosome segregation and SAC signalling in *mps1-3* cells without bringing back Mps1 to kinetochores. Second, Spc105 phosphorylation and Bub1 kinetochore localisation, which are severely impaired in *mps1-3* mutant cells, are restored in the suppressors. Third, constitutive binding of Bub1 to Spc105 is sufficient to rescue considerably chromosome missegregation and partly SAC signalling in *mps1-3* cells at restrictive temperature. The incomplete rescue of SAC activation is not surprising, given that Mps1 plays additional roles in the SAC, such as promoting Bub1 and Mad1 phosphorylation [19,20]. Along this line, it is worth noting that the *spc105-18* and *GLC7-24* suppressors, which restore a normal SAC response in

mps1-3 cells, also restore wild-type Mad1 (but not Bub1) hyperphosphorylation upon nocodazole treatment.

The idea that a common molecular mechanism based on Knl1/Spc105 phosphorylation would underlie the role of Mps1 in both SAC and chromosome biorientation was previously proposed in fission yeast. Indeed, phospho-mimicking mutations in the MELT repeats of Spc7 (the fission yeast homologue of Knl1/Spc105) were shown to partially suppress the chromosome biorientation defects of *mps1Δ* cells [18]. However, in fission yeast Mps1 is not essential for viability, and *mps1Δ* cells experience only modest chromosome missegregation [18]. Thus, our data gathered in an organism where Mps1 is critical for chromosome biorientation and with the aid of an unbiased genetic screen largely extend and strengthen this idea.

Despite our data strongly argue that Spc105 is a critical Mps1 substrate for the error correction pathway, we cannot rule out that other Mps1 substrates contribute to this process. Further experiments will help refining the precise mechanism underlying the control of chromosome segregation by Mps1.

The N-terminal region of Knl1 and Bub1 was previously shown to stimulate Aurora B kinase activity at kinetochores and increase the turnover of erroneous kinetochore–microtubule attachments [89–91]. Furthermore, Bub1 has been involved in chromosome biorientation through phosphorylation of histone H2A and Sgo1 accumulation at pericentromeres [66,78,92,93]. Sgo1, in turn, enhances CPC activity in the error correction mechanism [71,74,94]. Consistent with the idea that Mps1 is required for Bub1 recruitment to kinetochores, Sgo1 co-localisation with kinetochores is compromised in *mps1* mutants (ref. [8] and our data). Our data suggest, however, that impaired Sgo1 kinetochore localisation does not fully account for the chromosome biorientation defects of *mps1-3* cells. Indeed, Sgo1 centromeric recruitment is weakened, but not abolished, in *mps1-3* cells and the *mps1-3* mutation and *SGO1* deletion are synthetically lethal. Furthermore, mutations in the CPC centromere-targeting subunit Sli15 that rescue the sickness of *sgo1Δ* and *bub1Δ* cells [80] have no ameliorating effects on the lethality and chromosome segregation defects of *mps1-3* cells at high temperature. Finally, phosphorylation of the Aurora B kinetochore target Dam1 is unaffected in *mps1-3* cells, suggesting that the error correction defects of this mutant are not caused by reduced Aurora B kinase activity. Thus, although Mps1 could promote chromosome biorientation partly through the Bub1-Sgo1-CPC axis, it must have at least one additional function in this process. Consistent with this hypothesis, Bub1 and Sgo1 are not essential proteins, unlike Mps1, and their deletion leads to milder chromosome segregation defects than *mps1-3* cells at restrictive temperature. One intriguing possibility that is supported by our genetic results is that Mps1 could directly harness PP1 activity at kinetochores. In this scenario, Mps1 would master two opposing activities, acting indirectly on the CPC and perhaps more directly on PP1, thereby allowing the highest accuracy of bipolar attachments. This hypothesis would also explain why the *spc105* and *GLC7* suppressors isolated in our screen rescue the lethality and chromosome segregation defects of *mps1-3* cells considerably better than artificial recruitment of Bub1 to Spc105. Whether and how Mps1 controls PP1 activity at kinetochores will be an important subject for future investigations.

In sum, our data provide experimental support to the hypothesis that a single sensory device may be used for both error correction of faulty kinetochore–microtubule attachments and SAC signalling [89,95]. Given the evolutionary conservation of the players involved, it is very likely that Mps1 promotes SAC activation and chromosome biorientation through a common mechanism also in other organisms.

Materials and Methods

Yeast strains, plasmids and growth conditions

All yeast strains (Appendix Table S1) are congenic to or at least four times backcrossed to W303 (*ade2-1, trp1-1, leu2-3,112, his3-11 and 15 ura3*).

One-step tagging techniques were used to generate 3HA-, 3PK-, GFP- and mCherry-tagged proteins at the C-terminus. The *CEN5::tetO2X224 (12.6 kB) tetR-GFP* strain was a generous gift from T. Tanaka [43]; *BUB1-GFP* from P. de Wulf; *MTW1-Tomato* from A. Marston [68]; *GFP-TUB1* from A. Straight [96]; *mCherry-TUB1* from A. Amon [97]; *PDS1-myc18* from K. Nasmyth [98]; *spc105-RASA* and *GLC7-spc105-RASA* mutants from H. Funabiki and F. Cross [28]; *SGO1-GFP* and *CEN5::tetO2X112* (1.4 kB) *tetR-GFP* from E. Schwob; and *ura3::URA3::tetOX224* (35 kB) *tetR-GFP* from K. Nasmyth. The *sli15-ΔNterm* (*sli15Δ2-228*) and *sli15-6A* plasmids (pCC253 and pCC297) were a gift of C. Campbell [80] and were integrated at the *SLI15* locus by cutting with HindII and SalI, respectively.

The *mps1-3* mutant was obtained by hydroxylamine-induced mutagenesis of an *MPS1*-bearing plasmid and selection of temperature-sensitive mutants through plasmid shuffling [99]. The *mps1-3* allele (entire coding sequence) together with 480 bp of 5′ UTR and 900 bp of 3′ UTR was cloned as an EcoRI/SalI fragment in the integrative plasmid pFL34 to generate pSP1041 and integrated at the *MPS1* locus by the Pop-in/Pop-out method [100].

The *SPC105-GBD*-bearing plasmid (pSP1530) was generated by cloning in KpnI/HindIII of Yiplac204 a KpnI/PfoI fragment containing *SPC105* promoter and part of the coding region from plasmid SB1884 [15] together with a PfoI/HindIII *SPC105* synthetic gene (aa 61–386 of Spc105) carrying the GBD domain after aa 130 (pSP1516). *SPC105-GBD* was integrated at the *SPC105* locus by digesting pSP1530 with BglII. This generates a partial duplication of *SPC105*, with full-length *SPC105-GBD* gene followed by a truncated *spc105* allele (aa 1–386).

The *GALs-MPS1* plasmid (pSP149) was constructed by amplifying a DNA fragment comprising 30 bp of *MPS1* 5′ UTR, its CDS and 105 bp of 3′ UTR by PCR from W303 genomic DNA with primers SP127 and SP129, followed by its cloning into EcoRI/XhoI of a pRS416 harbouring the attenuated *GALs* promoter [101]. Growth of wild-type cells carrying the *GALs-MPS1* construct is unaffected (data not shown), in contrast to high-level overexpression of *MPS1* that causes a SAC-dependent metaphase arrest [62].

The *GAL1-GST-MPS1* plasmid (pSP228) was constructed by amplifying *MPS1* by PCR with primers SP238 and SP239 and cloning it into pEG(KT) [102] after cutting SmaI/HindIII. The *GAL1-GST-mps1-3* plasmid (pSP1202) was generated by replacing a BspEI/XbaI fragment of pSP228 internal to *MPS1* coding region by the same fragment containing the *mps1-3* mutation from pSP1041.

The plasmids for expression of His-tagged Mps1 and Mps1-3 in bacteria (pSP1575, pSP1576) were generated by amplifying

the coding sequence of *MPS1/mps1-3* by PCR with primers MP1124-MP1125, followed by cloning into EcoRI/HindIII of pPROEX-HTa.

The plasmid for expression of His-tagged Spc105 N-terminus (aa 1–320) in *Escherichia coli* (pSP1571) was generated by PCR-amplifying part of the coding sequence of *SPC105* with primers MP1126-1127, followed by cloning into BamHI/PstI of pPROEX-HTa.

Yeast cultures were grown at 25–30°C, in either SD medium (6.7 g/l yeast nitrogen base without amino acids) supplemented with the appropriate nutrients or YEP (1% yeast extract, 2% bactopeptone, 50 mg/l adenine) medium. Raffinose was supplemented to 2% (SD-raffinose or YEPR), glucose to 2% (SD-glucose or YEPD), and galactose to 1% (SD-raffinose/galactose or YEPRG). Cells were synchronised in G1 by alpha factor (4 μg/ml) in YEP medium containing the appropriate sugar at 25°C. G1 arrest was monitored under a transmitted light microscope, and cells were released in fresh medium (typically after 120–135 min of alpha factor treatment) at 34°C, unless otherwise specified, after being collected by centrifugation at 2,000 *g* followed by one wash with YEP containing the appropriate sugar. Nocodazole was used at 15 μg/ml.

Primers used in this study for gene tagging: sequences in bold anneal to the tag-bearing cassette

SP84 (tagging *BUB1* with *3HA::K.l.URA3;* fwd)
ACGTAATTCTAAGCATTGAAGAGGAGTTATCACATTTTCAATAT
AAGGGGAAACCGTCAAGGAGATTT**TCCGGTTCTGCTGCTAG**

SP85 (tagging *BUB1* with *3HA::K.l.URA3;* rev)
GTCATTGCTATGGAATCTGGCAGGACACCAAAAAGTCACCTAT
GCGGGAGATGAAGGCATATTTATTCA**CCTCGAGGCCAGAAGAC**

SP96 (tagging *MPS1* with *3HA::K.l.URA3;* fwd)
CATATATCACAAGATGATCTCAATGATGTGGTAGACACTGTTTT
AAGGAAATTTGCAGATTACAAAATT**TCCGGTTCTGCTGCTAG**

SP97 (tagging *MPS1* with *3HA::K.l.URA3;* rev)
CATGCATGGCAAACTCTAAATGTATTTATGTTCATAACTGGCAC
ATGCTTTTCTTCCTTATGCGGCTCTT**CCTCGAGGCCAGAAGAC**

SP134 (tagging *MAD1* with *3HA::K.l.URA3;* fwd)
GATAGAGGTCAACTTCCGTGCTTTTTGGCAACAATAACATTGCG
TCTGTGGGAACAGCGACAAGCCAAA**TCCGGTTCTGCTGCTAG**

SP135 (tagging *MAD1* with *3HA::K.l.URA3;* rev)
ATGTCAGCGGATAGGAGTTTATCATATTATAAAACCGATTACT
ATTATCTATTAGAAATGTATATACAC**CCTCGAGGCCAGAAGAC**

MP560 (tagging *SPC97* with *mCherry::HPHMX*; fwd)
GTTCTTTACTCTATAGTACCTCCTCGCTCAGCATCTGCTTCTTCC
CAAAGA**GGTCGACGGATCCCCGGG**

MP561 (tagging *SPC97* with *mCherry::HPHMX*; rev)
GATTCCACTTTCCGCAAGTTGGTGCACGTCGTTAGTGACATAAC
GCCGCGT**ATCGATGAATTCGAGCTCG**

MP629 (tagging *mps1-3* with *3HA::K.l.URA3;* fwd)
CTCAATGATGTGGTAGACACTGTTTTAAGGAAATTTGCAGATTA
CAAAATT**TCCGGTTCTGCTGCTAG**

MP630 (tagging *mps1-3* with *3HA::K.l.URA3;* rev)
ATGTATTTATGTTCATAACTGGCACATGCTTTTCTTCCTTATGC
GGCTCTT**CCTCGAGGCCAGAAGAC**

MP761 (tagging *MPS1* with *6Gly-eGFP::kanMX*; fwd)
CTCAATGATGTGGTAGACACTGTTTTAAGGAAATTTGCAGATT
ACAAAATTGGGGGAGGCGGGGGTGGA**GGTGACGGTGCTGGTTTA**

MP762 (tagging *MPS1* with *6Gly-eGFP::kanMX*; rev)
ATGTATTTATGTTCATAACTGGCACATGCTTTTCTTCCTTATGC
GGCTCTT**TCGATGAATTCGAGCTCG**

MP763 (tagging *SPC105* with *3PK::K.l.HIS3;* fwd)
AGTGGAGTTCTTCCTTCATTTACGAAAAGTAGAATACATTTAGA
GTTTACG**TCCGGTTCTGCTGCTAG**

MP764 (tagging *SPC105* with *3PK::K.l.HIS3;* rev)
AAAAAAAAGTGATGAGATATTACTAGTCATCGTTGTCCTATTA
TAAACACT**CCTCGAGGCCAGAAGAC**

MP894 (tagging *DAM1* with *3PK::K.l.HIS3;* fwd)
TCTGTTGCAAAGAAAACTGAAAAAAAAATAAATACAAGGCCCC
CCTTCAGA**TCCGGTTCTGCTGCTAG**

MP895 (tagging *DAM1* with *3PK::K.l.HIS3;* rev)
CTAGCGATATATTTTGTGAGGAGGATAATTCTTTGGTTGGGTT
GGGCGTAG**CCTCGAGGCCAGAAGAC**

MP900 (tagging *SNF1* with *3PK::K.l.HIS3;* fwd)
CATTTAACAACAAAACTAATTATGGAATTAGCCGTTAACAGTC
AAAGCAAT**TCCGGTTCTGCTGCTAG**

MP901 (tagging *SNF1* with *3PK::K.l.HIS3;* rev)
ACGATACATAAAAAAAAGGGAACTTCCATATCATTCTTTTACG
TTCCACCA**CCTCGAGGCCAGAAGAC**

MP940 (tagging *SLI15* with *3HA::K.l.URA3;* fwd)
AATCCTAGGCTAAACAGGTTGAAACCGCGTCAAATTGTGCCCA
AAAGGTCT**TCCGGTTCTGCTGCTAG**

MP941 (tagging *SLI15* with *3HA::K.l.URA3;* rev)
CTTGATTTAATGTTAACCAGTTTGAATTTTTCTTTTCTGGGGTA
ATCGAAT**CCTCGAGGCCAGAAGAC**

MP1024 (tagging *BUB3* with *eGFP::kanMX*; fwd)
ACTATTGAACTAAACGCAAGTTCAATATACATAATATTTGACTA
TGAGAAC**GGGGGAGGCGGGGGTGGAGGTGACGGTGCTGGTTTA**

MP1025 (tagging *BUB3* with *eGFP::kanMX*; rev)
AATTTTTTTTCTGGAATGTTCTATCATACTACACGAATCTTCAC
GAAGATA**TCGATGAATTCGAGCTCG**

MP1128 (tagging *MTW1* with *GBD::kanMX*; fwd)
GTTAGTATAGATATTGAAGAGCCTCAATTGGATTTACTTGATG
ATGTGTTA**CGTACGCTGCAGGTCGAC**

MP1129 (tagging *MTW1* with *GBD::kanMX*; rev)
ATTCGTGAATACATACATCATATCATAGCACATACTTTTTCCCA
CTTTATA**ATCGATGAATTCGAGCTCG**

Primers used in this study for cloning: sequences in bold indicate the restriction sites

SP127 (to clone *MPS1*, **EcoRI**)
CG**GAATTC**CTGCAAGAACTGGATGATCTC

SP129 (to clone *MPS1*, **XhoI**)
CCG**CTCGAG**CGGTGTAAAAAAGAGTTGATC

SP238 (cloning of *GAL1-GST-MPS1*; fwd)
TCCCCCGGGATCAACAAACTCATTCCATGATTAG

SP239 (cloning of *GAL1-GST-MPS1*; rev)
CCCAAGCTTAAGTATTCAGTGTCTGTGTCG

MP1124 (cloning of *MPS1*, **EcoRI**; fwd)
ACTTA**GAATTC**TCAACAAACTCATTCCATGATTATG

MP1125 (cloning of *MPS1*, **HindIII**; rev)
ACTTA**AAGCTT**CTAAATTTTGTAATCTGCAAATTTC

MP1126 (cloning N-ter*SPC105*, **BamHI**; fwd)
ACTTA**GGATCC**AATGTGGATGAAAGAAGCCG

MP1127 (cloning N-ter*SPC105*, **PstI**; rev)
ACTTA**CTGCAG**CTAGTCAAAGTTTGTCTGTATTTGCG

Microscopy

Scoring of GFP-tagged chromatid separation was carried out on cells fixed in 100% ethanol at −20°C. After two washes with PBS, cells were laid between a glass slide and a coverslip and imaged by fluorescence microscopy (Epifluorescent widefield Zeiss Axioimager Z1 controlled by the Metamorph software). *Z*-stacks (11 planes, 0.3 μm spaced) were max-projected before scoring.

To detect spindle formation and elongation, alpha-tubulin immunostaining was performed on formaldehyde-fixed cells using the YOL34 monoclonal antibody (1:100; MCA78S AbDSerotec, Raleigh, NC), followed by indirect immunofluorescence using CY2-conjugated anti-rat antibody (1:100; 31645 Pierce Chemical Co.).

For time-lapse video microscopy, cells were mounted on 1% agarose pads in SD medium on Fluorodishes (World Precision Instruments) and filmed at controlled temperature with a 100× 1.45 NA oil immersion objective mounted on a Spinning disk CSU-X1 Andor Nikon Eclipse Ti microscope coupled to an iXon Ultra camera controlled by the Andor iQ3 software. Z-stacks of 10 planes were acquired every 2–4 min with a step size of 0.5 μm (Figs 1G, 3G, 4C, and 5A, Movie EV1), 0.3 μm (Appendix Fig S8A) or 0.67 μm (Appendix Fig S1A).

Images of Sgo1-GFP (Appendix Fig S8A) have been deconvolved using the software Huygens using the following settings: background = 200; ratio signal/noise = 4; and iterations = 5.

Budding index was scored under a transmitted light microscope on cells fixed with 70% ethanol and treated for FACS analysis. Percentage of nuclear division was determined on the same samples after DNA staining with propidium iodide under a fluorescence microscope using a CY3 filter.

FACS analysis of DNA contents

For DNA quantification by fluorescence-activated cell sorting (FACS), 1–2 × 10^7 cells were collected, spun at 10,000 *g* and fixed with 1 ml of 70% ethanol for at least 30 min at RT. After one wash with 50 mM Tris–Cl pH 7.5, cells were resuspended in 0.5 ml of the same buffer containing 0.05 ml of a preboiled 10 mg/ml RNAse solution and incubated overnight at 37°C. The next day cells were spun at 10,000 *g* and resuspended in 0.5 ml of 5 mg/ml pepsin freshly diluted in 55 mM HCl. After 30-min incubation at 37°C, cells were washed with FACS buffer (200 mM Tris–Cl pH 7.5, 200 mM NaCl, 78 mM $MgCl_2$) and resuspended in the same buffer containing 50 μg/ml propidium iodide. After a short sonication, samples were diluted (1:20–1:10) in 1 ml of 50 mM Tris–Cl pH 7.5 and analysed with a FACSCalibur device (BD Biosciences). 10,000 events were scored for each sample and plotted after gating out the debris.

Protein extracts, Western blotting and kinase assays

For TCA protein extracts, 10–15 ml of cell culture in logarithmic phase (OD_{600} = 0.5–1) were collected by centrifugation at 2,000 *g*, washed with 1 ml of 20% TCA and resuspended in 100 μl of 20% TCA before breakage of cells with glass beads (diameter 0.5–0.75 mm) on a Vibrax VXR (IKA). After addition of 400 μl of 5% TCA, lysates were centrifuged for 10 min at 845 *g*. Protein precipitates were resuspended in 100 μl of 3× SDS sample buffer (240 mM Tris–Cl pH 6.8, 6% SDS, 30% glycerol, 2.28 M β-mercaptoethanol, 0.06% bromophenol blue), denatured at 99°C for 3 min and loaded on SDS–PAGE after elimination of cellular debris by centrifugation (5 min at 20,000 *g*).

Proteins were wet-transferred on Protran membranes (Schleicher and Schuell) overnight at 0.2 A and probed with monoclonal anti-HA 12CA5 (1:5,000); anti-PK (alias anti-V5; MCA1360 AbDSerotec, 1:3,000); polyclonal anti-Cdc5 (sc-6733 Santa Cruz, 1:3,000); anti-Clb2 (a generous gift from W. Zachariae, 1:2,000); anti-Pgk1 (Invitrogen Molecular Probes, 1:40,000); monoclonal anti-myc 9E10 (1:5,000); anti-phospho-AMPK (Thr172) (Cell Signalling, 1:1,000); and anti-GST (1:2,000, 27-4577-01 GE Healthcare). Antibodies were diluted in 5% low-fat milk (Regilait) dissolved in TBST. Secondary antibodies were purchased from GE Healthcare, and proteins were detected by a home-made enhanced chemiluminescence system.

For kinase assays with recombinant Mps1 proteins, Mps1/Mps1-3 and Spc105 have been purified as follows: BL21 DE3 cells transformed with pSP1571, pSP1575 or pSP1576 were grown in LB containing 50 μg/ml of ampicillin, 34 μg/ml of chloramphenicol and 1% glucose and induced with 0.2 mM IPTG at 16°C overnight. Cells were lysed in 50 mM Tris–Cl pH 8, 300 mM NaCl, 0.1% Tween 20 containing 1 mg/ml of lysozyme and a cocktail of protease inhibitors (Complete EDTA-free Roche). Cells were then sonicated 3× with 1′30″ cycles of 8″ pulses/8″ ice and extracts cleared at 30,000 *g* for 30′ at 4°C. Lysates were incubated 2 h with 1 ml of Ni-NTA agarose beads (Qiagen), pre-washed three times with 50 mM Tris–Cl pH 8, 300 mM NaCl, 0.1% Tween 20 and 10 mM imidazole at 4°C. After incubation with the extracts, the slurry was washed three times with 50 mM Tris–Cl pH 8, 300 mM NaCl, 0.1% Tween 20 and 20 mM imidazole and loaded on Polyprep columns (Bio-Rad). Fractions of 0.5 ml were eluted with 50 mM Tris–Cl pH 8, 300 mM NaCl and 250 mM imidazole and quantified by Nanodrop. The most concentrated fractions were washed and concentrated through the use of Amicon Ultra filter units (10 kDa cut-off for Spc105 and 50 kDa cut-off for Mps1) to finally have them in 50 mM Tris–Cl pH 8, 50 mM NaCl. Glycerol was added to the final concentration of 20%. Protein concentration was quantified by loading them on SDS–PAGE along with a BSA standard curve followed by staining with Coomassie blue. Kinase assays were performed at 34°C for different times in 25 μl of a reaction mix containing 50 mM Tris–Cl pH 7.5, 10 mM $MgCl_2$, 0.5 mM DTT, 10 μM ATP, 1 μl ATP-γ^{P33} 3,000 Ci/mmol and 80 μg/ml MBP. 75 ng of Spc105 N-term fragment and 1 μg Mps1/Mps1-3 kinases were used for each assay. Reactions were stopped using 7 μl of 3× SDS sample buffer (described in TCA extracts). Samples were then boiled 3 min at 95°C and loaded on SDS–PAGE. The gel was then dried and exposed on autoradiography films.

Native yeast protein extracts for kinase assays were performed by collecting cells in logarithmic phase (OD_{600} = 1) grown in -Ura RG at 30°C, centrifuging at 2,000 *g* and washing with 1 ml of cold 10 mM Tris–Cl pH 7.5. Cells were then broken in 50 mM Tris–Cl pH 7.5, 50 mM NaCl, 0.2% Triton X-100 containing a cocktail of protease inhibitors (Complete EDTA-free Roche) and phosphatase inhibitors (PhosSTOP Roche). Lysates were cleared at 20,000 *g* for 10 min at 4°C. The equivalent of 6 OD_{600}/assay was incubated on a nutator for 2 h at 4°C with 50 μl of Glutathione Sepharose 4 Fast

Flow (GE Healthcare) beads pre-washed with the above buffer. After incubation with the extracts, beads were spun down at 4°C at 845 *g*, washed twice with the same buffer without protease and phosphatase inhibitors, twice with the same buffer containing 0.1% of Triton X-100, twice with the same buffer without Triton X-100 and once with 50 mM Tris–Cl pH 7.5, 10 mM $MgCl_2$ and 0.5 mM DTT. Kinase assays were performed as above using 2 μg of MBP as exogenous substrate.

Chromosome loss assay

This assay is based on the loss of heterozygosity of the *MAT* locus, carried by chromosome III [42]. Briefly, wild-type diploid cells are heterozygous *MATa/MATalpha* and cannot mate unless they lose one copy of the *MAT* locus through mutations, chromosome rearrangements or chromosome loss. Cells were grown overnight at 25°C, and their concentration was measured at the time of inoculation and the day after to calculate the number of cell divisions. 2×10^7 diploid Met^+ cells were incubated 4 h at RT with an excess (2×10^8) of MATalpha *met4* tester cells in 400 μl of YEPD. 10 μl of the suspension was then diluted to plate 500 cells on −Met plates (where only the Met^+ diploids can form colonies) to calculate the percentage of viable (i.e. colony-forming); the remaining cells were plated on minimal SD plates (MIN), where only triploids, generated from the mating of diploids with the haploid tester cells, can grow. Plates have been incubated at 25°C. Frequency of chromosome loss has been calculated as follows: {[(no. of colonies on MIN/2×10^7)/fraction of viable cells]/no. of cellular divisions}. We note that with this assay we likely underestimate the real frequencies of chromosome loss because our measurements do not take into account the frequency of mating for each strain, which probably is much lower than 100%.

Suppressor screen

2.6×10^7 *mps1-3* cells were plated on YEPD and incubated at 34°C for 3–5 days until colonies' appearance. The isolated spontaneous suppressors were then characterised by classical genetic tests to distinguish intragenic from extragenic mutations, recessive from dominant mutations, and to group the suppressors in complementation/allelic groups. Genomic DNA was extracted from one representative suppressor for each complementation/allelic group and sent for whole genome sequencing to identify the mutated genes. The identity of the suppressing mutations was confirmed by classical genetics. Targeted gene re-sequencing approaches were used to identify the suppressing mutations in the other extragenic suppressors.

Viability test

Cells were grown at 25°C to 2×10^6 cells/ml and then serially diluted to plate 200 cells/plate in duplicate (wild-type, *mps1-3 SPC105-GBD BUB1-GFP* and *mps1-3 SPC105-GBD BUB3-GFP*) or 200, 500 and 1,000 cells/plate in duplicate for *mps1-3* cells ($t = 0$). Cells were then shifted to 34°C, withdrawn every hour, serially diluted to plate 200 cells/plate in duplicate (wild-type, *mps1-3 SPC105-GBD BUB1-GFP* and *mps1-3 SPC105-GBD BUB3-GFP*) or 200, 500 and 1,000 cells/plate in duplicate for *mps1-3* cells. Plates were incubated at 25°C until colony appearance. The number of colonies at each time point (average values of the duplicates) was divided by the number of colonies at $t = 0$ to obtain percentages of viability.

ChIP-seq analysis

100 ml of cells (concentration 10^7 cells/ml) was fixed in 1% formaldehyde for 30′ at RT with shaking and then transferred ON at 4°C. Cells were then spun down 3 min at 2,000 *g* at 4°C and washed three times with TBS. Cells were resuspended in 0.4 ml of 50 mM Hepes-KOH pH 7.5, 140 mM NaCl, 1 mM EDTA, 1% Triton X-100, 0.1% Na-deoxycholate containing a cocktail of protease inhibitors (Complete EDTA-free Roche) and 1 mM PMSF, followed by cell breakage through a Multi-beads shaker (Yasui-Kikai) at 0°C. Lysates were eluted in 15 ml Falcon tubes (centrifuged twice at 3,000 rpm for 1 min at 4°C), transferred in 1.5 Eppendorf tube, centrifuged at 2,500 *g* 1 min at 4°C and sonicated through a Sonifier Branson 2508 (5–7 cycles of 15 s, tune 1.5 with centrifugation of 5,000 rpm for 1 min between each cycle). Sonicated lysates were then centrifuged for 5 min at 21,000 *g* at 4°C. Supernatants were recovered. 10 μl of lysates was withdrawn at this stage (=Inputs). For immunoprecipitations (IPs), 60 μl of Protein G-dynabeads pre-washed twice with PBS containing 5 mg/ml BSA and pre-adsorbed with 3 μg Babco 16B12 anti-HA antibody was added to each lysate and incubated overnight at 4°C on a nutator. IPs were then washed twice with ice-cold 50 mM Hepes-KOH pH 7.5, 140 mM NaCl, 1 mM EDTA, 1% Triton X-100, and 0.1% Na-deoxycholate; twice with ice-cold 50 mM Hepes-KOH pH 7.5, 500 mM NaCl, 1 mM EDTA, 1% Triton X-100, and 0.1% Na-deoxycholate; twice with ice-cold 10 mM Tris–Cl pH 8, 250 mM LiCl, 0.5% NP-40, 0.5% Na-deoxycholate and 1 mM EDTA; and once with ice-cold TE (50 mM Tris–Cl pH 8, 1 mM EDTA pH 8). IPs were eluted at 65°C for 15 min with 50 μl of 50 mM Tris–Cl pH 8, 10 mM EDTA, 1% SDS, resuspended in 50 μl of TE/1% SDS and incubated overnight at 65°C to reverse crosslinking. IPs were then incubated at 37°C for 1 h with 100 μl of TE containing 10 μg of RNAseA and 2 h at 37°C with 2 μl of ProteinaseK 50 mg/ml. DNA was then purified with the Qiagen PCR purification kit. Libraries for Illumina sequencing have been then prepared following the NEBNext Ultra II DNA Library Prep Kit for Illumina. Sequencing results have been analysed using the DROMPA software [103].

Data availability

The ChIP-seq data from this publication have been deposited to the GEO NCBI database (https://www.ncbi.nlm.nih.gov/geo/) and assigned the identifier GSE144741.

Expanded View for this article is available online.

Acknowledgements

We are grateful to P. Pietruszka for initial experiments on *mps1-3*; to A. Amon, S. Biggins, C. Campbell, F. Cross, T. Davis, A. Desai, P. De Wulf, H. Funabiki, A. Hoyt, J. Lechner, A. Marston, K. Nasmyth, E. Schwob, S. Storchova, A. Straight, T. Tanaka and W. Zachariae for sharing reagents; to K. Fujiki for analysis of ChIP-seq data; to V. Georget, S. De Rossi and O. Faklaris for their invaluable help with live cell imaging; to A. Musacchio and E. Schwob for insightful

suggestions; to members of S. Piatti's laboratory for useful discussions; and to A. Musacchio and A. Abrieu for critical reading of the manuscript. We acknowledge the imaging core facility MRI, member of the national infrastructure France-BioImaging supported by the French National Research Agency (ANR-10-INBS-04, "Investments for the future"). This work has been supported by the Fondation pour la Recherche Médicale (DEQ20150331740 to S.P.) and by LabexEpiGenMed (PhD fellowship to G.B.). The authors declare no competing interests.

Author contributions

GB characterised the phenotypes of the *mps1-3* mutant, carried out the screen for suppressors and studied the effects of artificial Bub1 recruitment to kinetochores. GB and SP did the Mps1 kinase assays and live cell imaging. AC generated the *mps1-3* mutant. YA, YK and KS analysed the kinetochore localisation of Mps1 by ChIP-seq. GB and SP designed the work. GB made the figures with data provided by all contributing authors. SP supervised the work and acquired funding. SP and GB wrote the paper with input from all authors.

Conflict of interest

The authors declare that they have no conflict of interest.

References

1. Lampson MA, Grishchuk EL (2017) Mechanisms to avoid and correct erroneous kinetochore-microtubule attachments. *Biology* 6: 1
2. Bloom K, Yeh E (2010) Tension management in the kinetochore. *Curr Biol* 20: R1040 – R1048
3. Carmena M, Wheelock M, Funabiki H, Earnshaw WC (2012) The chromosomal passenger complex (CPC): from easy rider to the godfather of mitosis. *Nat Rev Mol Cell Biol* 13: 789 – 803
4. Jelluma N, Brenkman AB, van den Broek NJF, Cruijsen CWA, van Osch MHJ, Lens SMA, Medema RH, Kops GJPL (2008) Mps1 phosphorylates borealin to control Aurora B activity and chromosome alignment. *Cell* 132: 233 – 246
5. Jones MH, Huneycutt BJ, Pearson CG, Zhang C, Morgan G, Shokat K, Bloom K, Winey M (2005) Chemical genetics reveals a role for Mps1 kinase in kinetochore attachment during mitosis. *Curr Biol* 15: 160 – 165
6. Maure JF, Kitamura E, Tanaka TU (2007) Mps1 kinase promotes sister-kinetochore bi-orientation by a tension-dependent mechanism. *Curr Biol* 17: 2175 – 2182
7. Santaguida S, Tighe A, D'Alise AM, Taylor SS, Musacchio A (2010) Dissecting the role of MPS1 in chromosome biorientation and the spindle checkpoint through the small molecule inhibitor reversine. *J Cell Biol* 190: 73 – 87
8. Storchová Z, Becker JS, Talarek N, Kögelsberger S, Pellman D (2011) Bub1, Sgo1, and Mps1 mediate a distinct pathway for chromosome biorientation in budding yeast. *Mol Biol Cell* 22: 1473 – 1485
9. Saurin AT, van der Waal MS, Medema RH, Lens SMA, Kops GJPL (2011) Aurora B potentiates Mps1 activation to ensure rapid checkpoint establishment at the onset of mitosis. *Nat Commun* 2: 316
10. van der Waal MS, Saurin AT, Vromans MJM, Vleugel M, Wurzenberger C, Gerlich DW, Medema RH, Kops GJPL, Lens SMA (2012) Mps1 promotes rapid centromere accumulation of Aurora B. *EMBO Rep* 13: 847 – 854
11. Maciejowski J, Drechsler H, Grundner-Culemann K, Ballister ER, Rodriguez-Rodriguez J-A, Rodriguez-Bravo V, Jones MJK, Foley E, Lampson MA, Daub H *et al* (2017) Mps1 regulates kinetochore-microtubule attachment stability via the ska complex to ensure error-free chromosome segregation. *Dev Cell* 41: 143 – 156
12. Kalantzaki M, Kitamura E, Zhang T, Mino A, Novák B, Tanaka TU (2015) Kinetochore–microtubule error correction is driven by differentially regulated interaction modes. *Nat Cell Biol* 17: 421 – 433
13. Shimogawa MM, Graczyk B, Gardner MK, Francis SE, White EA, Ess M, Molk JN, Ruse C, Niessen S, Yates JR *et al* (2006) Mps1 phosphorylation of Dam1 couples kinetochores to microtubule plus ends at metaphase. *Curr Biol* 16: 1489 – 1501
14. Musacchio A (2015) The molecular biology of spindle assembly checkpoint signaling dynamics. *Curr Biol* 25: R1002 – R1018
15. London N, Ceto S, Ranish JA, Biggins S (2012) Phosphoregulation of Spc105 by Mps1 and PP1 regulates Bub1 localization to kinetochores. *Curr Biol* 22: 900 – 906
16. Primorac I, Weir JR, Chiroli E, Gross F, Hoffmann I, van Gerwen S, Ciliberto A, Musacchio A (2013) Bub3 reads phosphorylated MELT repeats to promote spindle assembly checkpoint signaling. *Elife* 2: e01030
17. Shepperd LA, Meadows JC, Sochaj AM, Lancaster TC, Zou J, Buttrick GJ, Rappsilber J, Hardwick KG, Millar JBA (2012) Phosphodependent recruitment of Bub1 and Bub3 to Spc7/KNL1 by Mph1 kinase maintains the spindle checkpoint. *Curr Biol* 22: 891 – 899
18. Yamagishi Y, Yang C-H, Tanno Y, Watanabe Y (2012) MPS1/Mph1 phosphorylates the kinetochore protein KNL1/Spc7 to recruit SAC components. *Nat Cell Biol* 14: 746 – 752
19. Ji Z, Gao H, Jia L, Li B, Yu H (2017) A sequential multi-target Mps1 phosphorylation cascade promotes spindle checkpoint signaling. *Elife* 6: e22513
20. London N, Biggins S (2014) Mad1 kinetochore recruitment by Mps1-mediated phosphorylation of Bub1 signals the spindle checkpoint. *Genes Dev* 28: 140 – 152
21. Mora-Santos MDM, Hervas-Aguilar A, Sewart K, Lancaster TC, Meadows JC, Millar JBA (2016) Bub3-Bub1 binding to Spc7/KNL1 toggles the spindle checkpoint switch by licensing the interaction of Bub1 with Mad1-Mad2. *Curr Biol* 26: 2642 – 2650
22. Moyle MW, Kim T, Hattersley N, Espeut J, Cheerambathur DK, Oegema K, Desai A (2014) A Bub1–Mad1 interaction targets the Mad1–Mad2 complex to unattached kinetochores to initiate the spindle checkpoint. *J Cell Biol* 204: 647 – 657
23. Zhang G, Kruse T, López-Méndez B, Sylvestersen KB, Garvanska DH, Schopper S, Nielsen ML, Nilsson J (2017) Bub1 positions Mad1 close to KNL1 MELT repeats to promote checkpoint signalling. *Nat Commun* 8: 15822
24. Bokros M, Gravenmier C, Jin F, Richmond D, Wang Y (2016) Fin1-PP1 helps clear spindle assembly checkpoint protein Bub1 from kinetochores in anaphase. *Cell Rep* 14: 1074 – 1085
25. Liu D, Vleugel M, Backer CB, Hori T, Fukagawa T, Cheeseman IM, Lampson MA (2010) Regulated targeting of protein phosphatase 1 to the outer kinetochore by KNL1 opposes Aurora B kinase. *J Cell Biol* 188: 809 – 820
26. Meadows JC, Shepperd LA, Vanoosthuyse V, Lancaster TC, Sochaj AM, Buttrick GJ, Hardwick KG, Millar JBA (2011) Spindle checkpoint silencing requires association of PP1 to both Spc7 and kinesin-8 motors. *Dev Cell* 20: 739 – 750
27. Pinsky BA, Nelson CR, Biggins S (2009) Protein phosphatase 1 regulates exit from the spindle checkpoint in budding yeast. *Curr Biol* 19: 1182 – 1187
28. Rosenberg JS, Cross FR, Funabiki H (2011) KNL1/Spc105 recruits PP1 to silence the spindle assembly checkpoint. *Curr Biol* 21: 942 – 947

29. Vanoosthuyse V, Hardwick KG (2009) A novel protein phosphatase 1-dependent spindle checkpoint silencing mechanism. *Curr Biol* 19: 1176 – 1181
30. Moura M, Osswald M, Leça N, Barbosa J, Pereira AJ, Maiato H, Sunkel CE, Conde C (2017) Protein phosphatase 1 inactivates Mps1 to ensure efficient spindle assembly checkpoint silencing. *Elife* 6: e25366
31. Ditchfield C, Johnson VL, Tighe A, Ellston R, Haworth C, Johnson T, Mortlock A, Keen N, Taylor SS (2003) Aurora B couples chromosome alignment with anaphase by targeting BubR1, Mad2, and Cenp-E to kinetochores. *J Cell Biol* 161: 267 – 280
32. Hauf S, Cole RW, LaTerra S, Zimmer C, Schnapp G, Walter R, Heckel A, van Meel J, Rieder CL, Peters JM (2003) The small molecule Hesperadin reveals a role for Aurora B in correcting kinetochore-microtubule attachment and in maintaining the spindle assembly checkpoint. *J Cell Biol* 161: 281 – 294
33. King EMJ, Rachidi N, Morrice N, Hardwick KG, Stark MJR (2007) Ipl1p-dependent phosphorylation of Mad3p is required for the spindle checkpoint response to lack of tension at kinetochores. *Genes Dev* 21: 1163 – 1168
34. Pinsky BA, Kung C, Shokat KM, Biggins S (2006) The Ipl1-Aurora protein kinase activates the spindle checkpoint by creating unattached kinetochores. *Nat Cell Biol* 8: 78 – 83
35. Kallio MJ, McCleland ML, Stukenberg PT, Gorbsky GJ (2002) Inhibition of aurora B kinase blocks chromosome segregation, overrides the spindle checkpoint, and perturbs microtubule dynamics in mitosis. *Curr Biol* 12: 900 – 905
36. Maldonado M, Kapoor TM (2011) Constitutive Mad1 targeting to kinetochores uncouples checkpoint signalling from chromosome biorientation. *Nat Cell Biol* 13: 475 – 482
37. Petersen J, Hagan IM (2003) *S. pombe* aurora kinase/survivin is required for chromosome condensation and the spindle checkpoint attachment response. *Curr Biol* 13: 590 – 597
38. Santaguida S, Vernieri C, Villa F, Ciliberto A, Musacchio A (2011) Evidence that Aurora B is implicated in spindle checkpoint signalling independently of error correction. *EMBO J* 30: 1508 – 1519
39. Vader G, Cruijsen CWA, van Harn T, Vromans MJM, Medema RH, Lens SMA (2007) The chromosomal passenger complex controls spindle checkpoint function independent from its role in correcting microtubule-kinetochore interactions. *Mol Biol Cell* 18: 4553 – 4564
40. Hewitt L, Tighe A, Santaguida S, White AM, Jones CD, Musacchio A, Green S, Taylor SS (2010) Sustained Mps1 activity is required in mitosis to recruit O-Mad2 to the Mad1-C-Mad2 core complex. *J Cell Biol* 190: 25 – 34
41. Weiss E, Winey M (1996) The *Saccharomyces cerevisiae* spindle pole body duplication gene MPS1 is part of a mitotic checkpoint. *J Cell Biol* 132: 111 – 123
42. Andersen MP, Nelson ZW, Hetrick ED, Gottschling DE (2008) A genetic screen for increased loss of heterozygosity in *Saccharomyces cerevisiae*. *Genetics* 179: 1179 – 1195
43. Tanaka T, Fuchs J, Loidl J, Nasmyth K (2000) Cohesin ensures bipolar attachment of microtubules to sister centromeres and resists their precocious separation. *Nat Cell Biol* 2: 492 – 499
44. Irniger S, Piatti S, Michaelis C, Nasmyth K (1995) Genes involved in sister chromatid separation are needed for B-type cyclin proteolysis in budding yeast [published erratum appears in Cell 1998 May 1;93 (3):487]. *Cell* 81: 269 – 278
45. Tanaka TU, Rachidi N, Janke C, Pereira G, Galova M, Schiebel E, Stark MJ, Nasmyth K (2002) Evidence that the Ipl1-Sli15 (Aurora kinase-INCENP) complex promotes chromosome bi-orientation by altering kinetochore-spindle pole connections. *Cell* 108: 317 – 329
46. Lauzé E, Stoelcker B, Luca FC, Weiss E, Schutz AR, Winey M (1995) Yeast spindle pole body duplication gene MPS1 encodes an essential dual specificity protein kinase. *EMBO J* 14: 1655 – 1663
47. Palframan WJ, Meehl JB, Jaspersen SL, Winey M, Murray AW (2006) Anaphase inactivation of the spindle checkpoint. *Science* 313: 680 – 684
48. Hayward D, Bancroft J, Mangat D, Alfonso-Pérez T, Dugdale S, McCarthy J, Barr FA, Gruneberg U (2019) Checkpoint signaling and error correction require regulation of the MPS1 T-loop by PP2A-B56. *J Cell Biol* 218: 3188 – 3199
49. Jelluma N, Dansen TB, Sliedrecht T, Kwiatkowski NP, Kops GJPL (2010) Release of Mps1 from kinetochores is crucial for timely anaphase onset. *J Cell Biol* 191: 281 – 290
50. Wang X, Yu H, Xu L, Zhu T, Zheng F, Fu C, Wang Z, Dou Z (2014) Dynamic autophosphorylation of Mps1 kinase is required for faithful mitotic progression. *PLoS ONE* 9: e104723
51. Rothbauer U, Zolghadr K, Muyldermans S, Schepers A, Cardoso MC, Leonhardt H (2008) A versatile nanotrap for biochemical and functional studies with fluorescent fusion proteins. *Mol Cell Proteomics* 7: 282 – 289
52. Aravamudhan P, Goldfarb AA, Joglekar AP (2015) The kinetochore encodes a mechanical switch to disrupt spindle assembly checkpoint signalling. *Nat Cell Biol* 17: 868 – 879
53. Hoyt MA, Totis L, Roberts BT (1991) *S. cerevisiae* genes required for cell cycle arrest in response to loss of microtubule function. *Cell* 66: 507 – 517
54. Li R, Murray AW (1991) Feedback control of mitosis in budding yeast. *Cell* 66: 519 – 531
55. Angus-Hill ML, Schlichter A, Roberts D, Erdjument-Bromage H, Tempst P, Cairns BR (2001) A Rsc3/Rsc30 zinc cluster dimer reveals novel roles for the chromatin remodeler RSC in gene expression and cell cycle control. *Mol Cell* 7: 741 – 751
56. Wu X, Tatchell K (2001) Mutations in yeast protein phosphatase type 1 that affect targeting subunit binding†. *Biochemistry* 40: 7410 – 7420
57. Rubenstein EM, McCartney RR, Zhang C, Shokat KM, Shirra MK, Arndt KM, Schmidt MC (2008) Access denied: Snf1 activation loop phosphorylation is controlled by availability of the phosphorylated threonine 210 to the PP1 phosphatase. *J Biol Chem* 283: 222 – 230
58. Kim J, Kang J, Chan CSM (1999) Sli15 associates with the Ipl1 protein kinase to promote proper chromosome segregation in *Saccharomyces cerevisiae*. *J Cell Biol* 145: 1381 – 1394
59. Nakajima Y, Cormier A, Tyers RG, Pigula A, Peng Y, Drubin DG, Barnes G (2011) Ipl1/Aurora-dependent phosphorylation of Sli15/INCENP regulates CPC–spindle interaction to ensure proper microtubule dynamics. *J Cell Biol* 194: 137 – 153
60. Francisco L, Wang W, Chan CS (1994) Type 1 protein phosphatase acts in opposition to IpL1 protein kinase in regulating yeast chromosome segregation. *Mol Cell Biol* 14: 4731 – 4740
61. Hsu JY, Sun ZW, Li X, Reuben M, Tatchell K, Bishop DK, Grushcow JM, Brame CJ, Caldwell JA, Hunt DF *et al* (2000) Mitotic phosphorylation of histone H3 is governed by Ipl1/aurora kinase and Glc7/PP1 phosphatase in budding yeast and nematodes. *Cell* 102: 279 – 291
62. Hardwick KG, Weiss E, Luca FC, Winey M, Murray AW (1996) Activation of the budding yeast spindle assembly checkpoint without mitotic spindle disruption. *Science* 273: 953 – 956
63. Hardwick KG, Murray AW (1995) Mad1p, a phosphoprotein component of the spindle assembly checkpoint in budding yeast. *J Cell Biol* 131: 709 – 720

64. Fraschini R, Beretta A, Sironi L, Musacchio A, Lucchini G, Piatti S (2001) Bub3 interaction with Mad2, Mad3 and Cdc20 is mediated by WD40 repeats and does not require intact kinetochores. *EMBO J* 20: 6648 – 6659
65. Gillett ES, Espelin CW, Sorger PK (2004) Spindle checkpoint proteins and chromosome-microtubule attachment in budding yeast. *J Cell Biol* 164: 535 – 546
66. Fernius J, Hardwick KG (2007) Bub1 kinase targets Sgo1 to ensure efficient chromosome biorientation in budding yeast mitosis. *PLoS Genet* 3: e213
67. Breit C, Bange T, Petrovic A, Weir JR, Müller F, Vogt D, Musacchio A (2015) Role of intrinsic and extrinsic factors in the regulation of the mitotic checkpoint kinase Bub1. *PLoS ONE* 10: e0144673
68. Nerusheva OO, Galander S, Fernius J, Kelly D, Marston AL (2014) Tension-dependent removal of pericentromeric shugoshin is an indicator of sister chromosome biorientation. *Genes Dev* 28: 1291 – 1309
69. Peplowska K, Wallek AU, Storchova Z (2014) Sgo1 regulates both condensin and Ipl1/Aurora B to promote chromosome biorientation. *PLoS Genet* 10: e1004411
70. Indjeian VB, Stern BM, Murray AW (2005) The centromeric protein Sgo1 is required to sense lack of tension on mitotic chromosomes. *Science* 307: 130 – 133
71. Kawashima SA, Tsukahara T, Langegger M, Hauf S, Kitajima TS, Watanabe Y (2007) Shugoshin enables tension-generating attachment of kinetochores by loading Aurora to centromeres. *Genes Dev* 21: 420 – 435
72. Rivera T, Ghenoiu C, Rodríguez-Corsino M, Mochida S, Funabiki H, Losada A (2012) *Xenopus* Shugoshin 2 regulates the spindle assembly pathway mediated by the chromosomal passenger complex: XSgo2 regulates the spindle assembly pathway mediated by CPC. *EMBO J* 31: 1467 – 1479
73. Vanoosthuyse V, Prykhozhij S, Hardwick KG (2007) Shugoshin 2 regulates localization of the chromosomal passenger proteins in fission yeast mitosis. *Mol Biol Cell* 18: 1657 – 1669
74. Verzijlbergen KF, Nerusheva OO, Kelly D, Kerr A, Clift D, de Lima Alves F, Rappsilber J, Marston AL (2014) Shugoshin biases chromosomes for biorientation through condensin recruitment to the pericentromere. *Elife* 3: e01374
75. García-Rodríguez LJ, Kasciukovic T, Denninger V, Tanaka TU (2019) Aurora B-INCENP localization at centromeres/inner kinetochores is required for chromosome bi-orientation in budding yeast. *Curr Biol* 29: 1536 – 1544.e4
76. Makrantoni V, Stark MJR (2009) Efficient chromosome biorientation and the tension checkpoint in *Saccharomyces cerevisiae* both require Bir1. *Mol Cell Biol* 29: 4552 – 4562
77. Fischböck-Halwachs J, Singh S, Potocnjak M, Hagemann G, Solis-Mezarino V, Woike S, Ghodgaonkar-Steger M, Weissmann F, Gallego LD, Rojas J *et al* (2019) The COMA complex interacts with Cse4 and positions Sli15/Ipl1 at the budding yeast inner kinetochore. *Elife* 8: e42879
78. Kawashima SA, Yamagishi Y, Honda T, Ishiguro K, Watanabe Y (2010) Phosphorylation of H2A by Bub1 prevents chromosomal instability through localizing shugoshin. *Science* 327: 172 – 177
79. Pereira G, Schiebel E (2003) Separase regulates INCENP-Aurora B anaphase spindle function through Cdc14. *Science* 302: 2120 – 2124
80. Campbell CS, Desai A (2013) Tension sensing by Aurora B kinase is independent of survivin-based centromere localization. *Nature* 497: 118 – 121
81. Cheeseman IM, Anderson S, Jwa M, Green EM, Kang J, Yates JR, Chan CSM, Drubin DG, Barnes G (2002) Phospho-regulation of kinetochore-microtubule attachments by the aurora kinase Ipl1p. *Cell* 111: 163 – 172
82. Krenn V, Musacchio A (2015) The Aurora B kinase in chromosome bi-orientation and spindle checkpoint signaling. *Front Oncol* 5: 225
83. Araki Y, Gombos L, Migueleti SPS, Sivashanmugam L, Antony C, Schiebel E (2010) N-terminal regions of Mps1 kinase determine functional bifurcation. *J Cell Biol* 189: 41 – 56
84. Chu MLH, Chavas LMG, Douglas KT, Eyers PA, Tabernero L (2008) Crystal structure of the catalytic domain of the mitotic checkpoint kinase Mps1 in complex with SP600125. *J Biol Chem* 283: 21495 – 21500
85. Fraschini R, Beretta A, Lucchini G, Piatti S (2001) Role of the kinetochore protein Ndc10 in mitotic checkpoint activation in *Saccharomyces cerevisiae*. *Mol Genet Genomics* 266: 115 – 125
86. Heinrich S, Windecker H, Hustedt N, Hauf S (2012) Mph1 kinetochore localization is crucial and upstream in the hierarchy of spindle assembly checkpoint protein recruitment to kinetochores. *J Cell Sci* 125: 4720 – 4727
87. Nijenhuis W, von Castelmur E, Littler D, De Marco V, Tromer E, Vleugel M, van Osch MHJ, Snel B, Perrakis A, Kops GJPL (2013) A TPR domain-containing N-terminal module of MPS1 is required for its kinetochore localization by Aurora B. *J Cell Biol* 201: 217 – 231
88. Zhu T, Dou Z, Qin B, Jin C, Wang X, Xu L, Wang Z, Zhu L, Liu F, Gao X *et al* (2013) Phosphorylation of microtubule-binding protein Hec1 by mitotic kinase Aurora B specifies spindle checkpoint kinase Mps1 signaling at the kinetochore. *J Biol Chem* 288: 36149 – 36159
89. Caldas GV, DeLuca KF, DeLuca JG (2013) KNL1 facilitates phosphorylation of outer kinetochore proteins by promoting Aurora B kinase activity. *J Cell Biol* 203: 957 – 969
90. Ricke RM, Jeganathan KB, Malureanu L, Harrison AM, van Deursen JM (2012) Bub1 kinase activity drives error correction and mitotic checkpoint control but not tumor suppression. *J Cell Biol* 199: 931 – 949
91. Ricke RM, Jeganathan KB, van Deursen JM (2011) Bub1 overexpression induces aneuploidy and tumor formation through Aurora B kinase hyperactivation. *J Cell Biol* 193: 1049 – 1064
92. Liu H, Qu Q, Warrington R, Rice A, Cheng N, Yu H (2015) Mitotic transcription installs Sgo1 at centromeres to coordinate chromosome segregation. *Mol Cell* 59: 426 – 436
93. Liu H, Jia L, Yu H (2013) Phospho-H2A and cohesin specify distinct tension-regulated Sgo1 pools at kinetochores and inner centromeres. *Curr Biol* 23: 1927 – 1933
94. Tsukahara T, Tanno Y, Watanabe Y (2010) Phosphorylation of the CPC by Cdk1 promotes chromosome bi-orientation. *Nature* 467: 719 – 723
95. Musacchio A (2011) Spindle assembly checkpoint: the third decade. *Philos Trans R Soc Lond B Biol Sci* 366: 3595 – 3604
96. Straight AF, Marshall WF, Sedat JW, Murray AW (1997) Mitosis in living budding yeast: anaphase A but no metaphase plate. *Science* 277: 574 – 578
97. Rock JM, Amon A (2011) Cdc15 integrates Tem1 GTPase-mediated spatial signals with Polo kinase-mediated temporal cues to activate mitotic exit. *Genes Dev* 25: 1943 – 1954
98. Alexandru G, Zachariae W, Schleiffer A, Nasmyth K (1999) Sister chromatid separation and chromosome re-duplication are regulated by different mechanisms in response to spindle damage. *EMBO J* 18: 2707 – 2721
99. Sikorski RS, Boeke JD (1991) *In vitro* mutagenesis and plasmid shuffling: from cloned gene to mutant yeast. *Methods Enzymol* 194: 302 – 318
100. Scherer S, Davis RW (1979) Replacement of chromosome segments with altered DNA sequences constructed *in vitro*. *Proc Natl Acad Sci USA* 76: 4951 – 4955

101. Mumberg D, Muller R, Funk M (1994) Regulatable promoters of *Saccharomyces cerevisiae*: comparison of transcriptional activity and their use for heterologous expression. *Nucleic Acids Res* 22: 5767 – 5768

102. Pierce BD, Wendland B (2009) Sequence of the yeast protein expression plasmid pEG(KT). *Yeast* 26: 349 – 353

103. Nakato R, Shirahige K (2018) Statistical analysis and quality assessment of ChIP-seq data with DROMPA. *Methods Mol Biol* 1672: 631 – 643